Atmospheric Boundary Layer in Complex Terrain

Joan Cuxart

University of the Balearic Islands
Dpt. de Física – Grup de Meteorologia

ECMWF, 7 November 2011, ECMWF-GABLS Workshop

1. Soil and vegetation

2. Terrain-induced LLJs

3. Slopes and depressions

4. Valley flows

5. Large Basins

Very-small scale ground heterogeneities

BLLAST, 21st June 2011

1. (Ts+/- dTs) at 4m x 2m spots (WUR)

2. Ts field in a 4 m x 2 m (WUR)

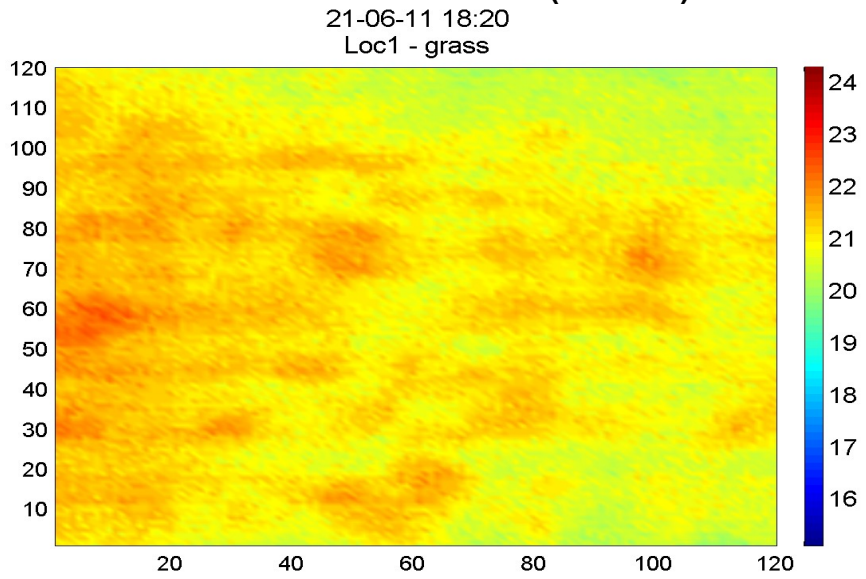

3. View of the surface at the square (UIB)

4. Soil Moisture (first 5 cm) UIB-CRA

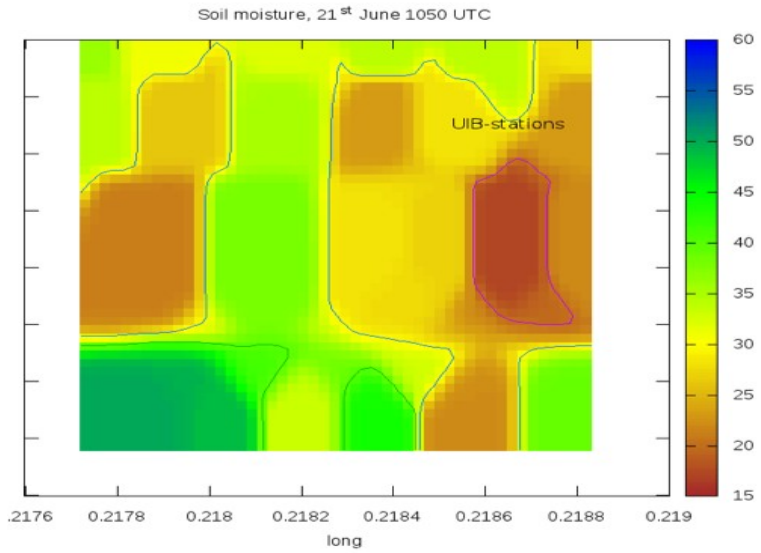

Ground complexity

Qg = - Ks dT/dz Ks varies between 0.1 (dry porous terrain) to 2.0 (saturated)

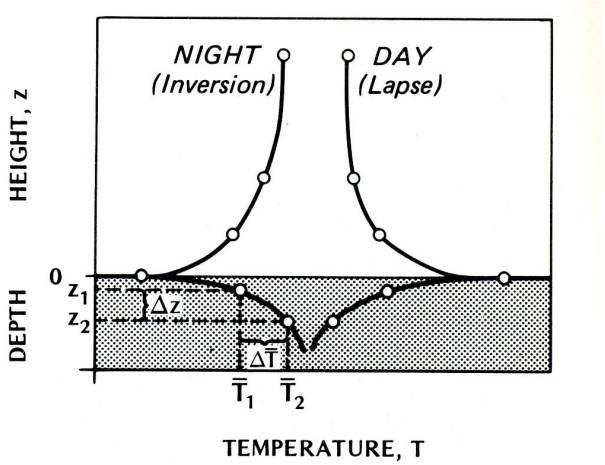

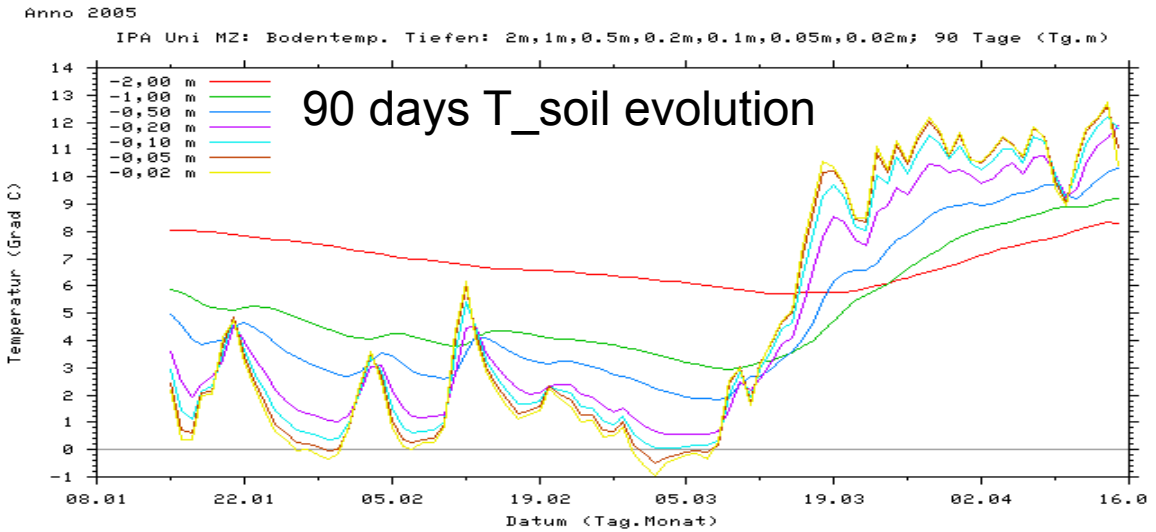

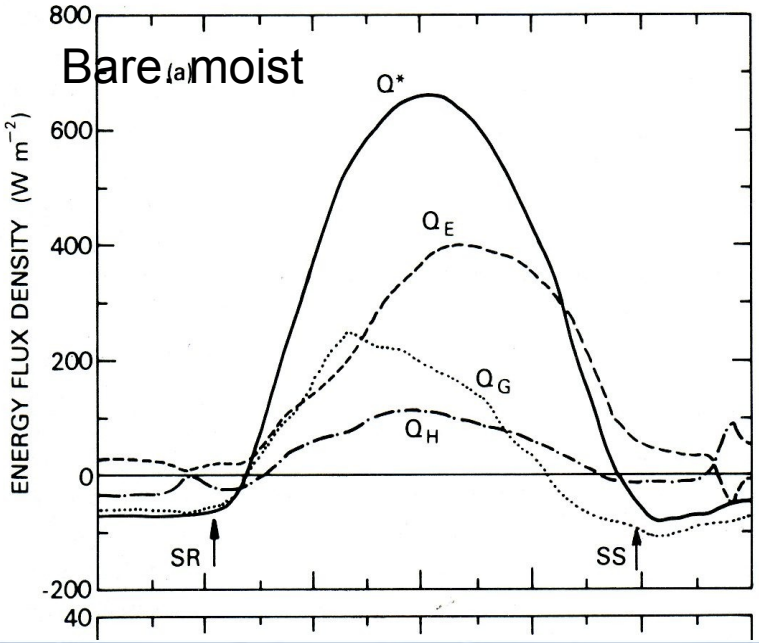

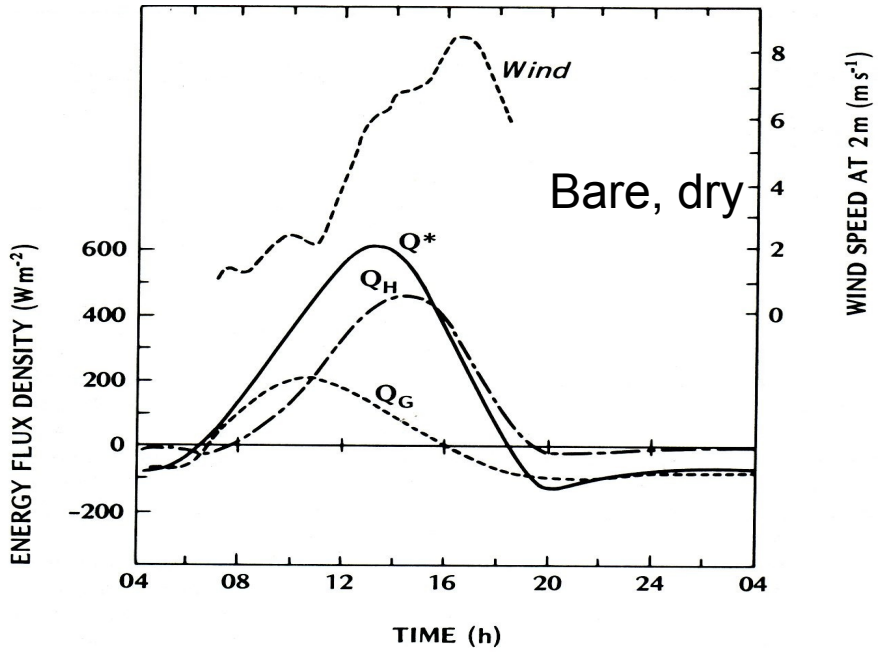

Sources: Oke (1978), University of Mainz (2005)

Vegetation (1)

1. LAI annual cycle dead and green grass

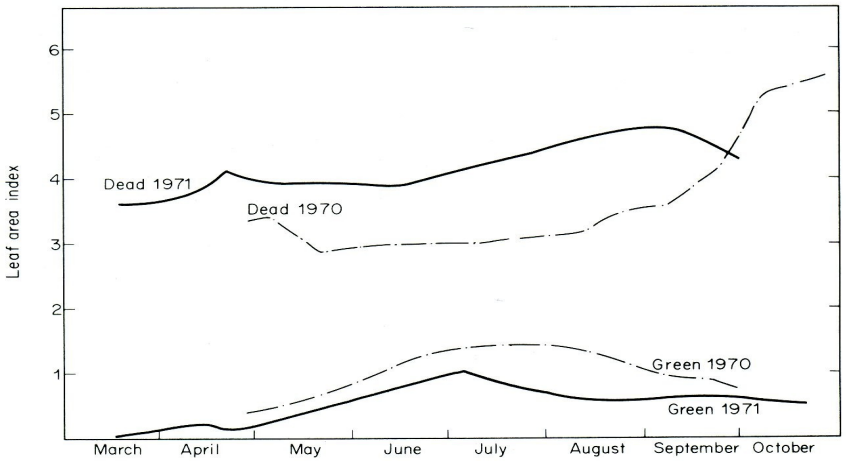

Fig. 5. Seasonal variation of green and dead leaf area indexes during the 1970 and 1971 growing seasons. Most of the data were estimated from biomass measurements (see Robins and Ripley, 1973).

2. LAI and H sunflower (growing season)

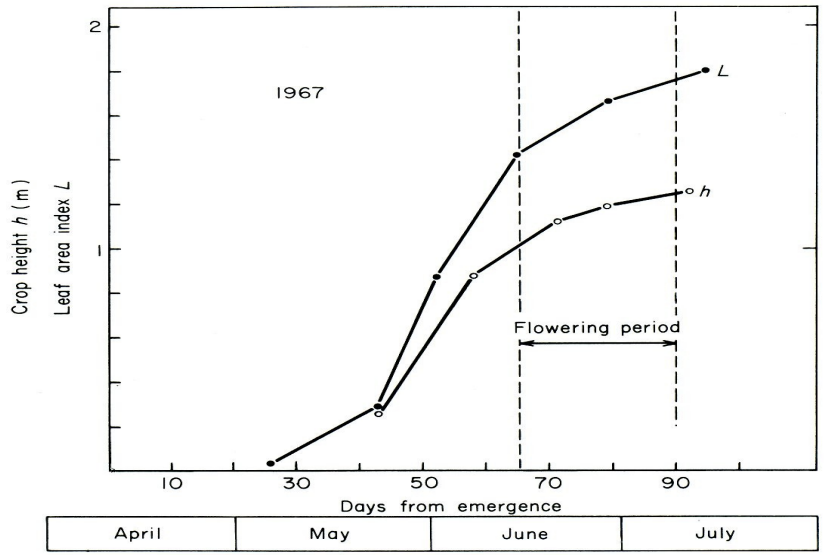

3. Night T of air, large and small leaves

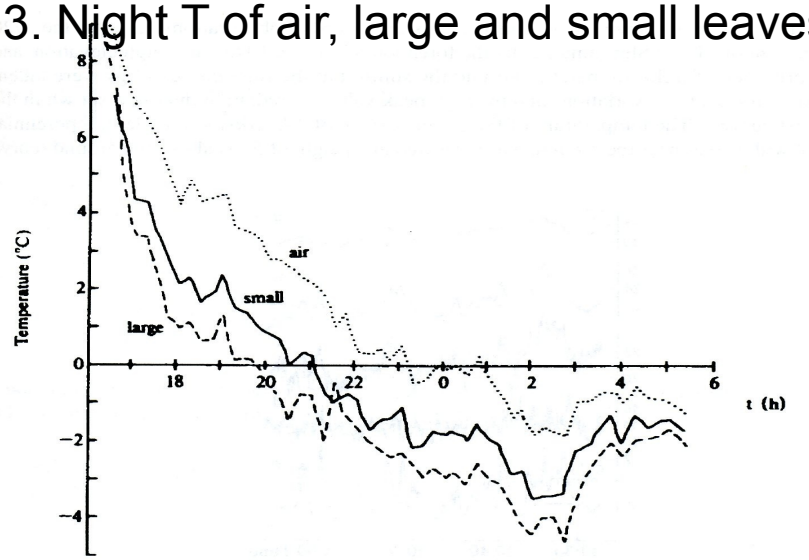

Figure 29-5. Time series of temperatures of air, small leaves (*E. viminalis*) and large leaves (*E. pauciflora*) at 100 mm above grass on 20-21 July 1984. (From R. Leuning and K. W. Cremer [2914])

4. Night T of grass and dry and wet soil

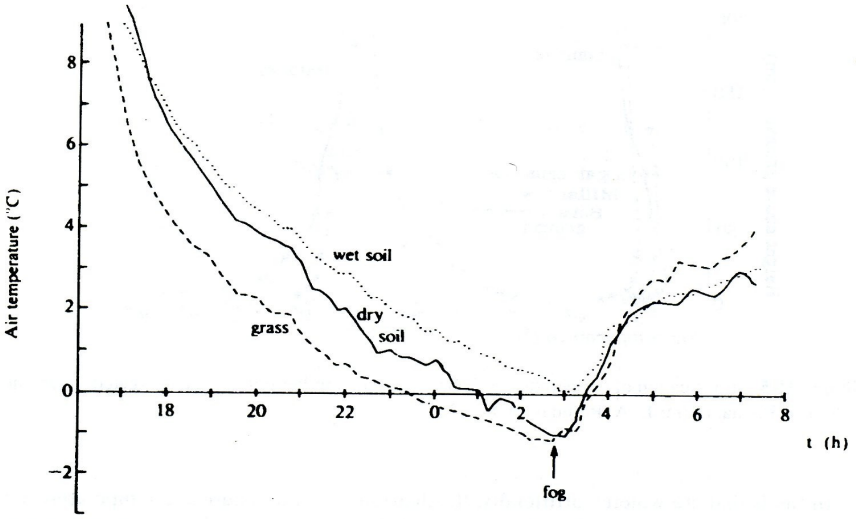

Figure 31-4. Time series of air temperatures measured at 5 mm above grass (dashed line), dry soil (solid line), and wet soil (dotted line) on 15-16 August 1984. (From R. Leuning and K. W. Cremer [2914])

Sources: Monteith (1976), Geiger et al (1995)

Vegetation (2)

1. Wind speed in/above the canopy

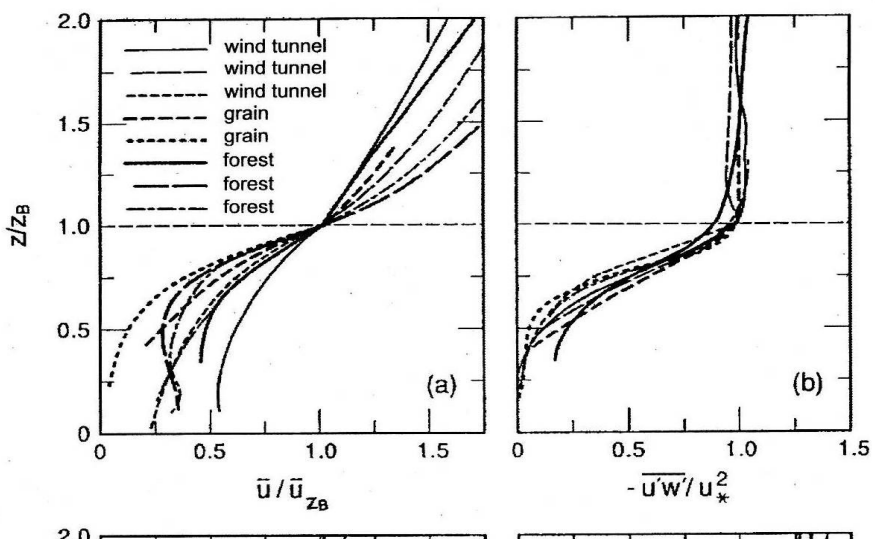

2. Thermal structure in/above the canopy

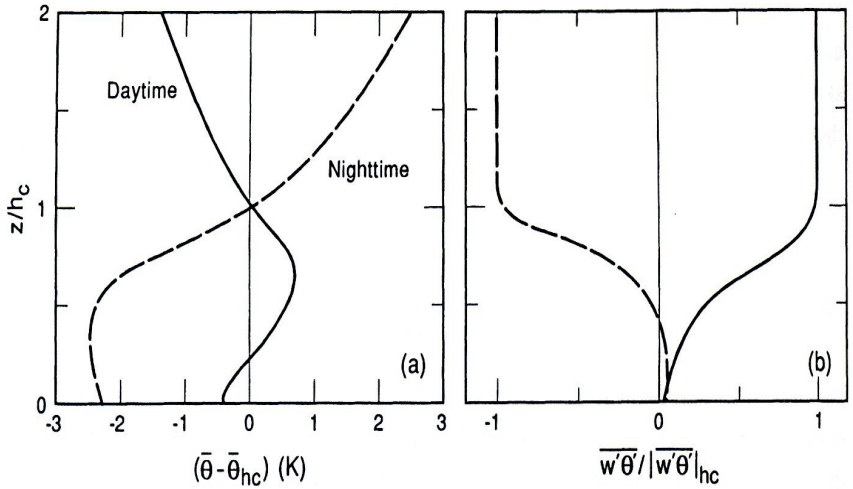

3. Ensemble view including radiation

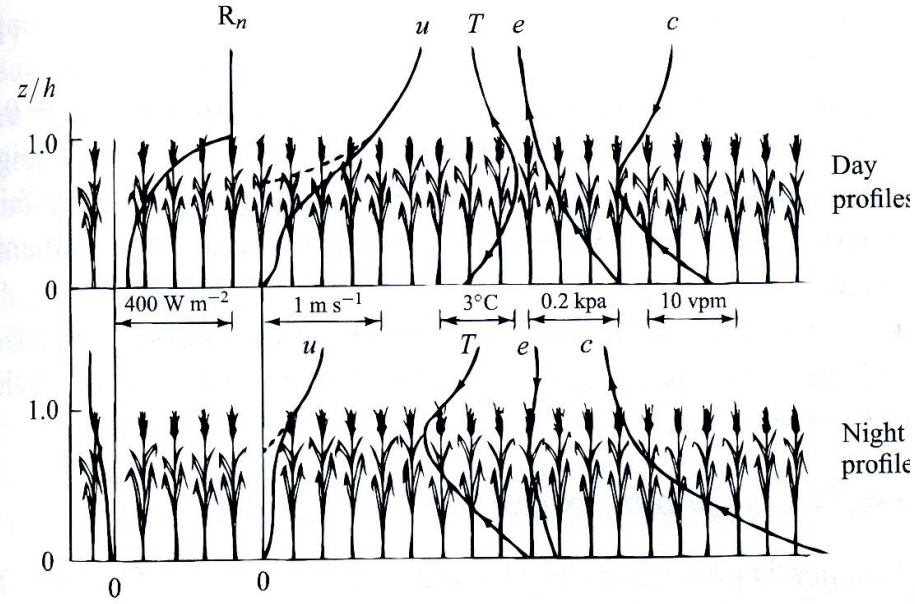

4. T evolution in the growing season

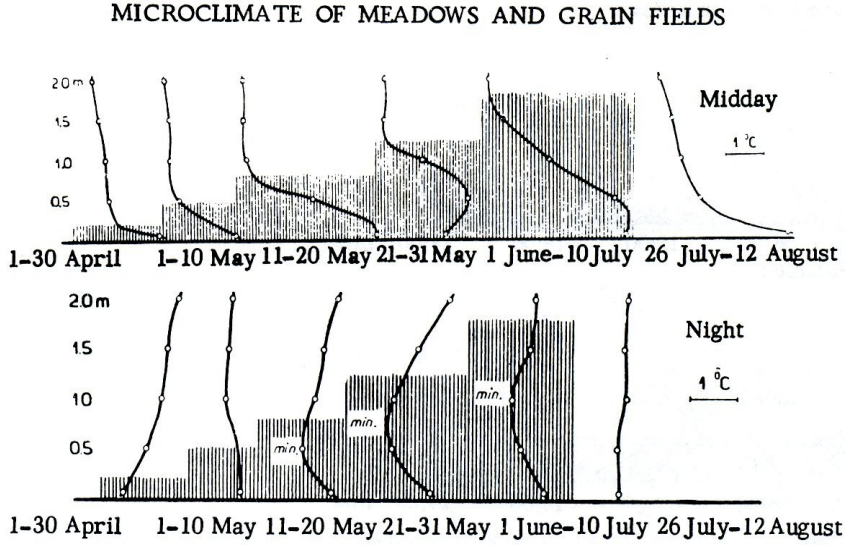

Sources: Kaimal & Finnigan 1994, Geiger et al 1995

Structure of a baroclinely generated LLJ (1)

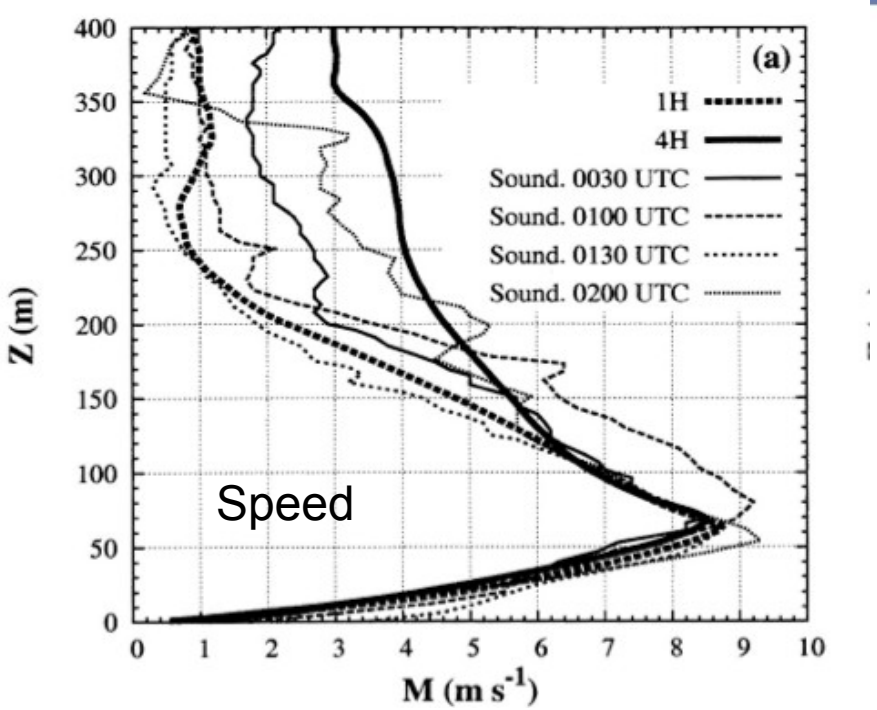

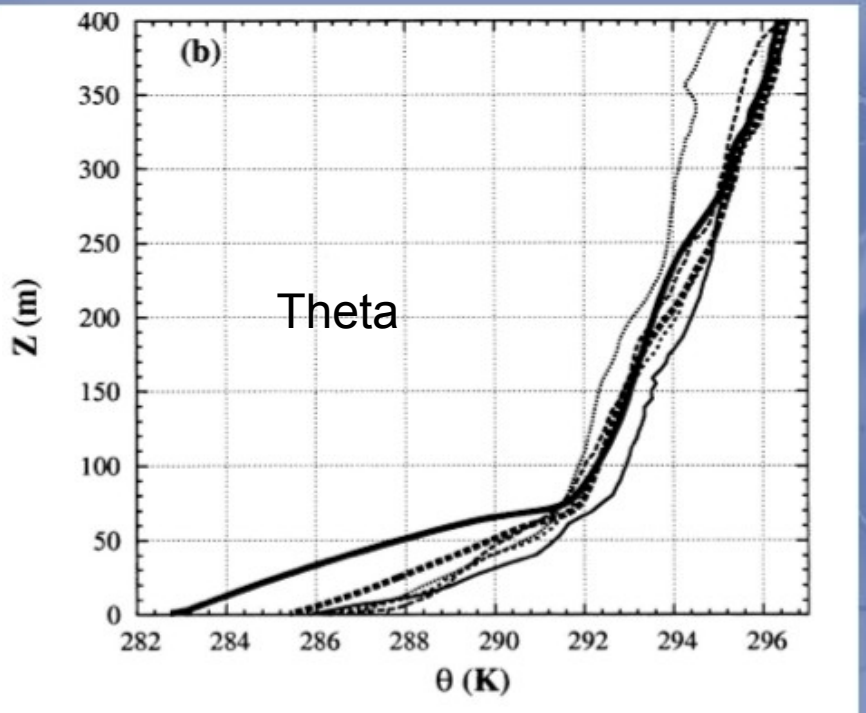

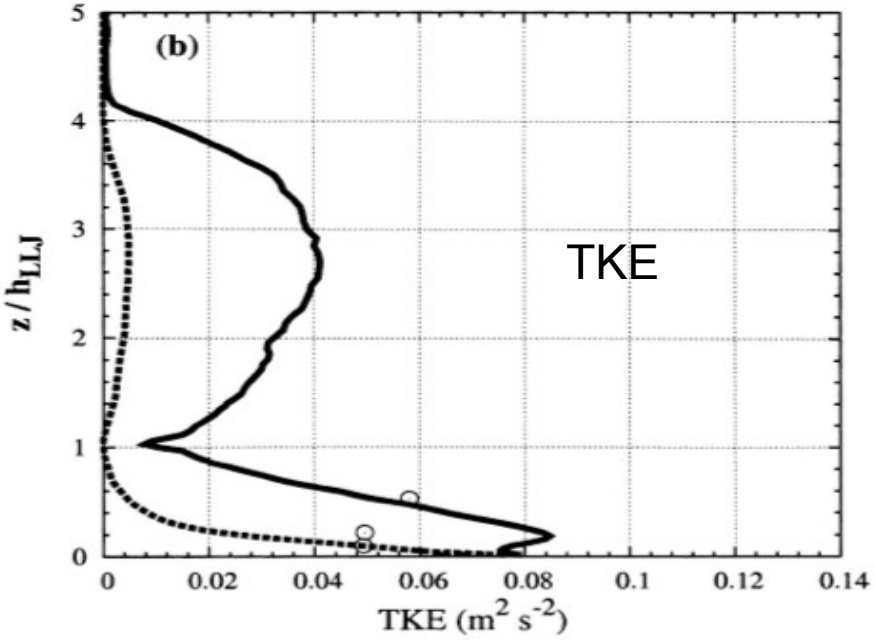

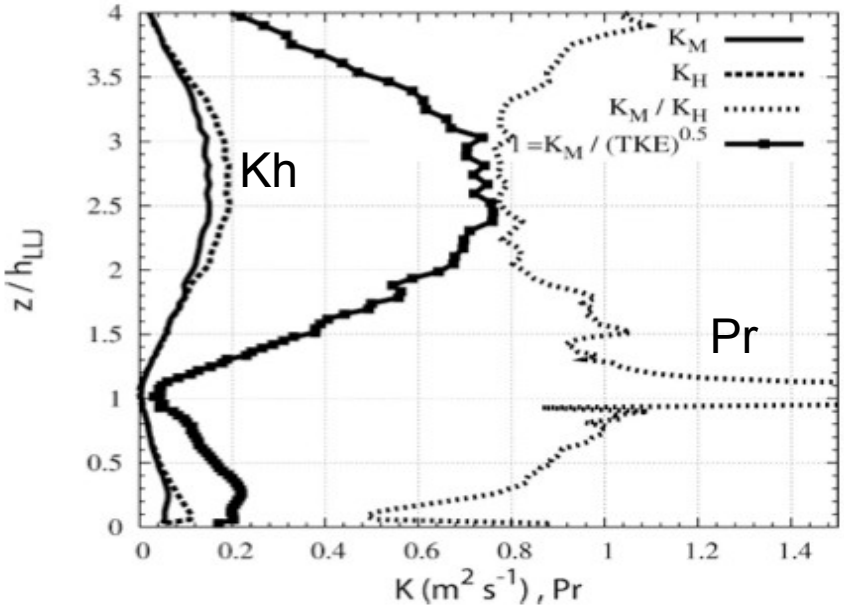

$$\frac{\partial V_g}{\partial z} = \frac{g}{ft}\vec{k} X \nabla_h T$$

(Cuxart & Jimenez, JAS 2007)

Structure of a baroclinely generated LLJ (2)

Run forced at the surface: intermittency

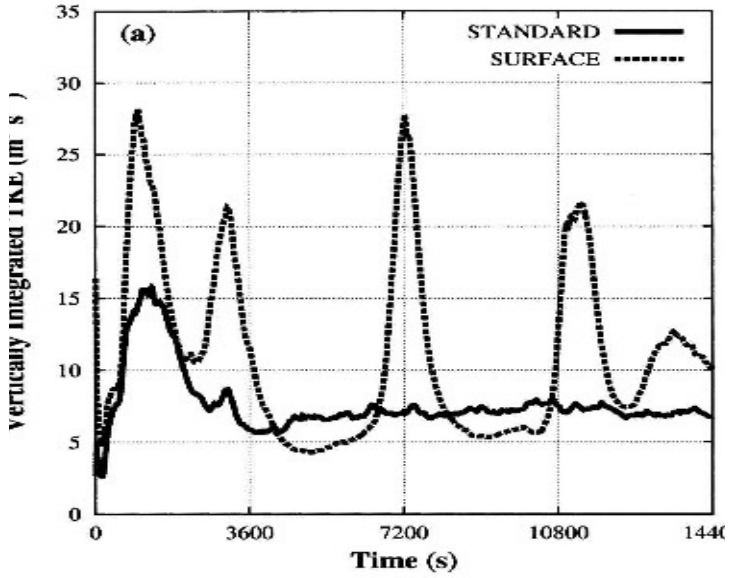

TKE evolution in a mixing event

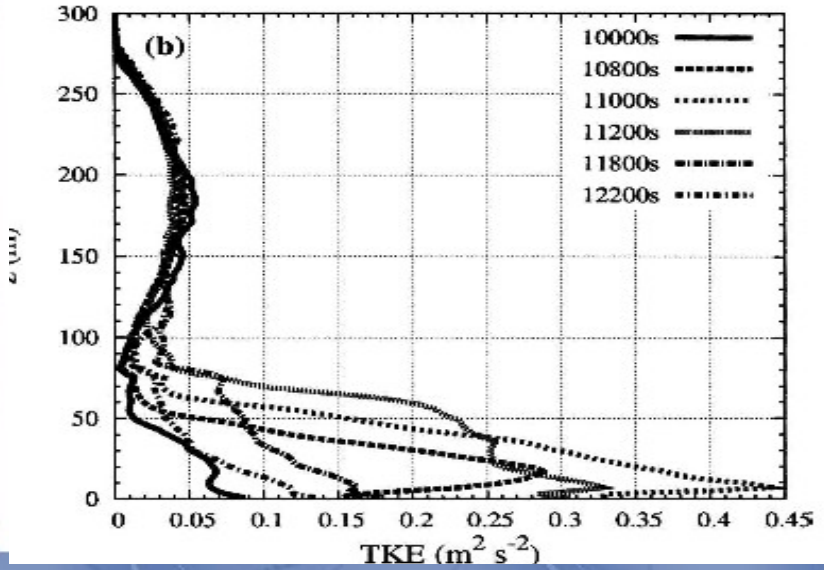

Mixing made in the intermittent events

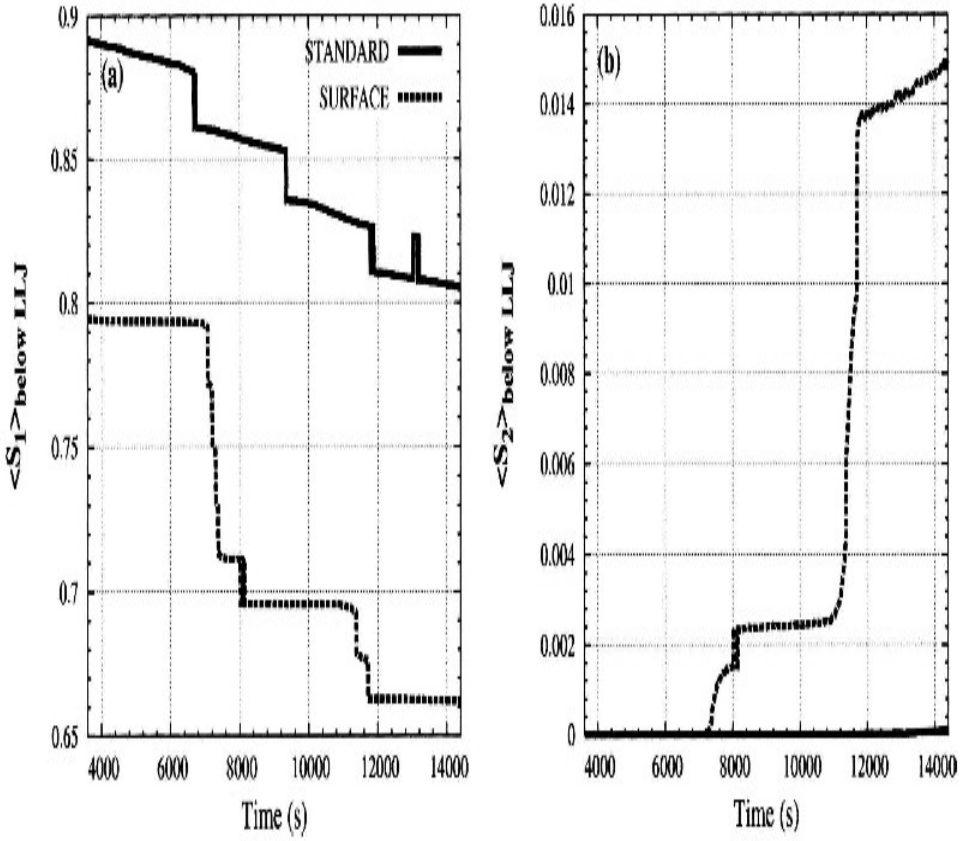

FIG. 9. Time series of the averaged scalar from the ground up to the LLJ height (h_{LLJ}): (a) S_1 and (b) S_2.

Source: Cuxart and Jimenez, 2007

Sloping terrain (1)

Mallorca slope

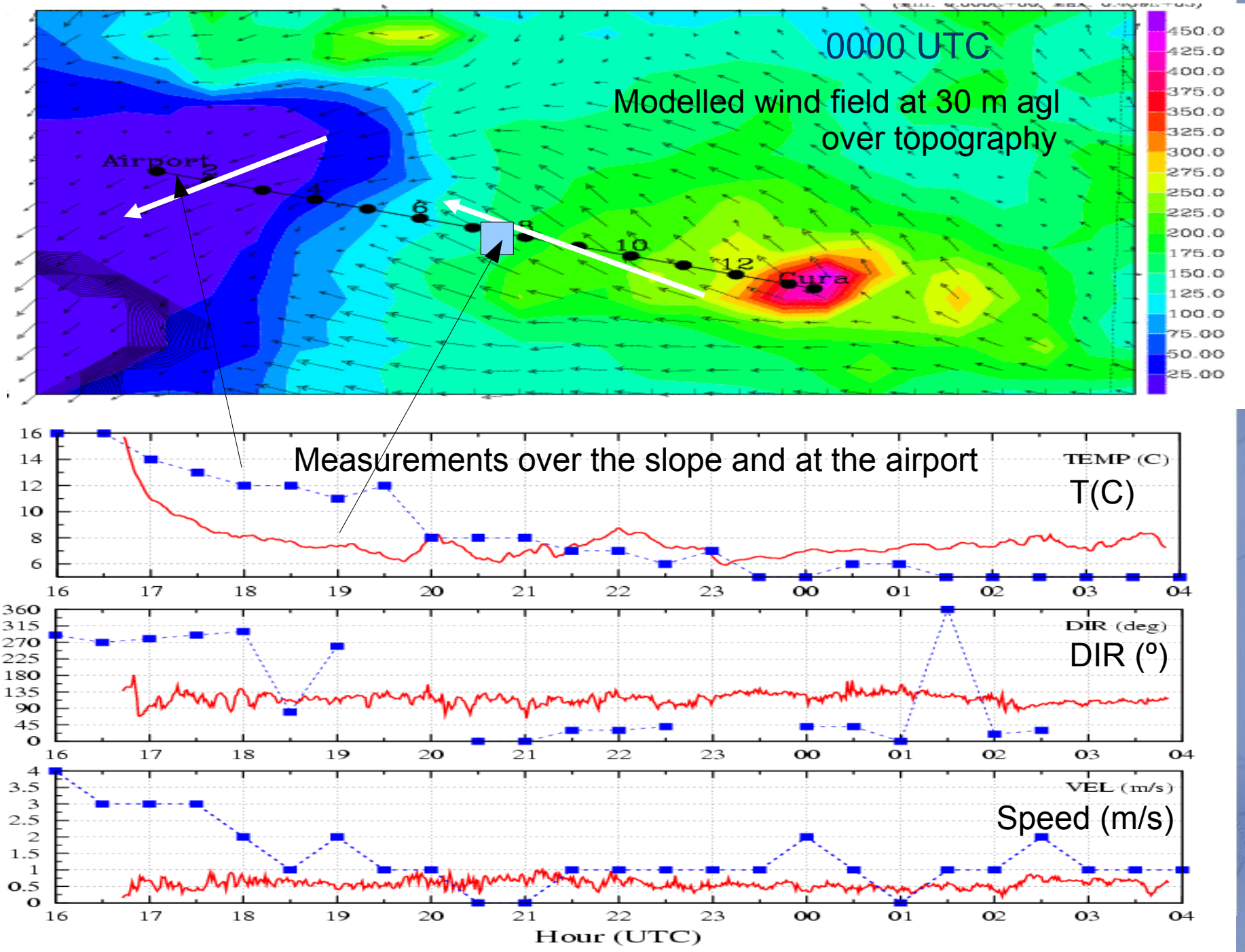

Sloping terrain (2)

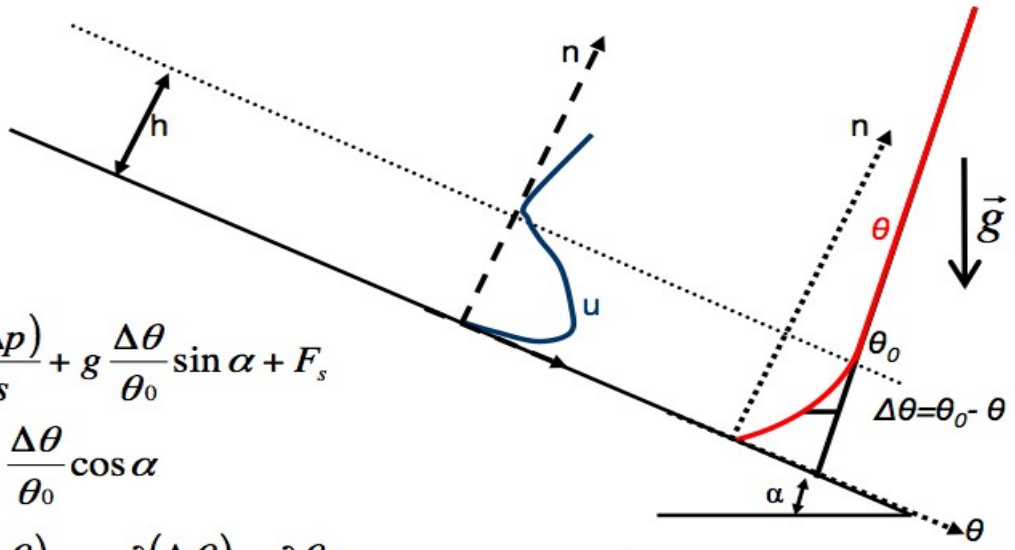

$$\begin{cases} \dfrac{Du}{Dt} = -\dfrac{1}{\rho_0}\dfrac{\partial(\Delta p)}{\partial s} + g\dfrac{\Delta\theta}{\theta_0}\sin\alpha + F_s \\ \dfrac{1}{\rho_0}\dfrac{\partial(\Delta p)}{\partial n} = -g\dfrac{\Delta\theta}{\theta_0}\cos\alpha \\ \dfrac{\partial(\Delta\theta)}{\partial t} + u\dfrac{\partial(\Delta\theta)}{\partial s} + w\dfrac{\partial(\Delta\theta)}{\partial n} + \dfrac{\partial\theta}{\partial z}(u\sin\alpha - w\cos\alpha) = L_c \end{cases}$$

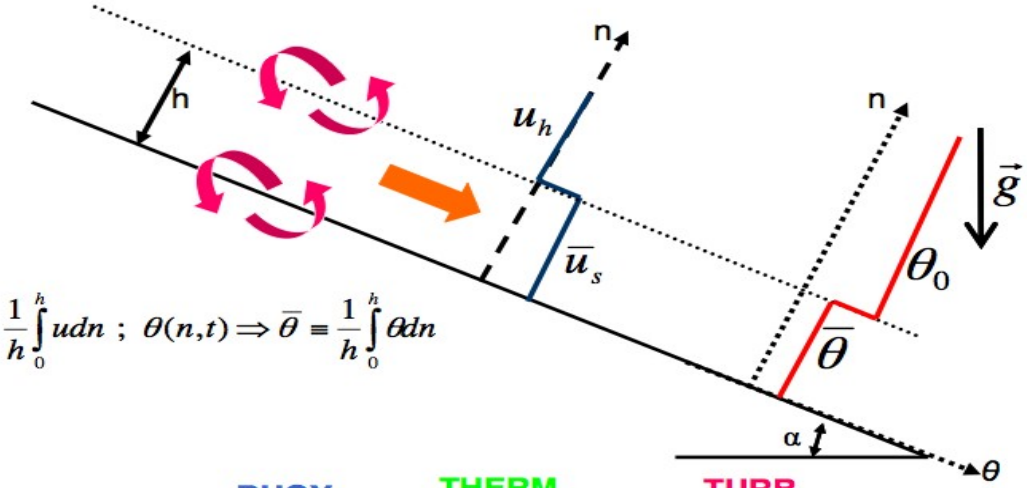

$$u(n,t) \Rightarrow \overline{u} \equiv \frac{1}{h}\int_0^h u\,dn \;;\; \theta(n,t) \Rightarrow \overline{\theta} \equiv \frac{1}{h}\int_0^h \theta\,dn$$

$$\underbrace{\frac{\partial\overline{u}_s}{\partial t}}_{\text{STOR}} = -\underbrace{\left(\overline{u}_s\frac{\partial\overline{u}_s}{\partial s} + \overline{w}_n\frac{u_h-\overline{u}_s}{h}\right)}_{\text{ADV}} + \underbrace{g\frac{\Delta\overline{\theta}}{\theta_0}\sin\alpha}_{\text{BUOY}} - \underbrace{\frac{gh}{\theta_0}\frac{\partial\left(h\Delta\overline{\theta}\right)}{\partial s}\cos\alpha}_{\text{THERM}} - \underbrace{\frac{\left(\overline{w'u'}\right)_h - \left(\overline{w'u'}\right)_{sfc}}{h}}_{\text{TURB}} + \underbrace{f\overline{v}}_{\text{COR}}$$

Sources: Mahrt (1982), Martinez and Cuxart (2009)

Sloping terrain (3)

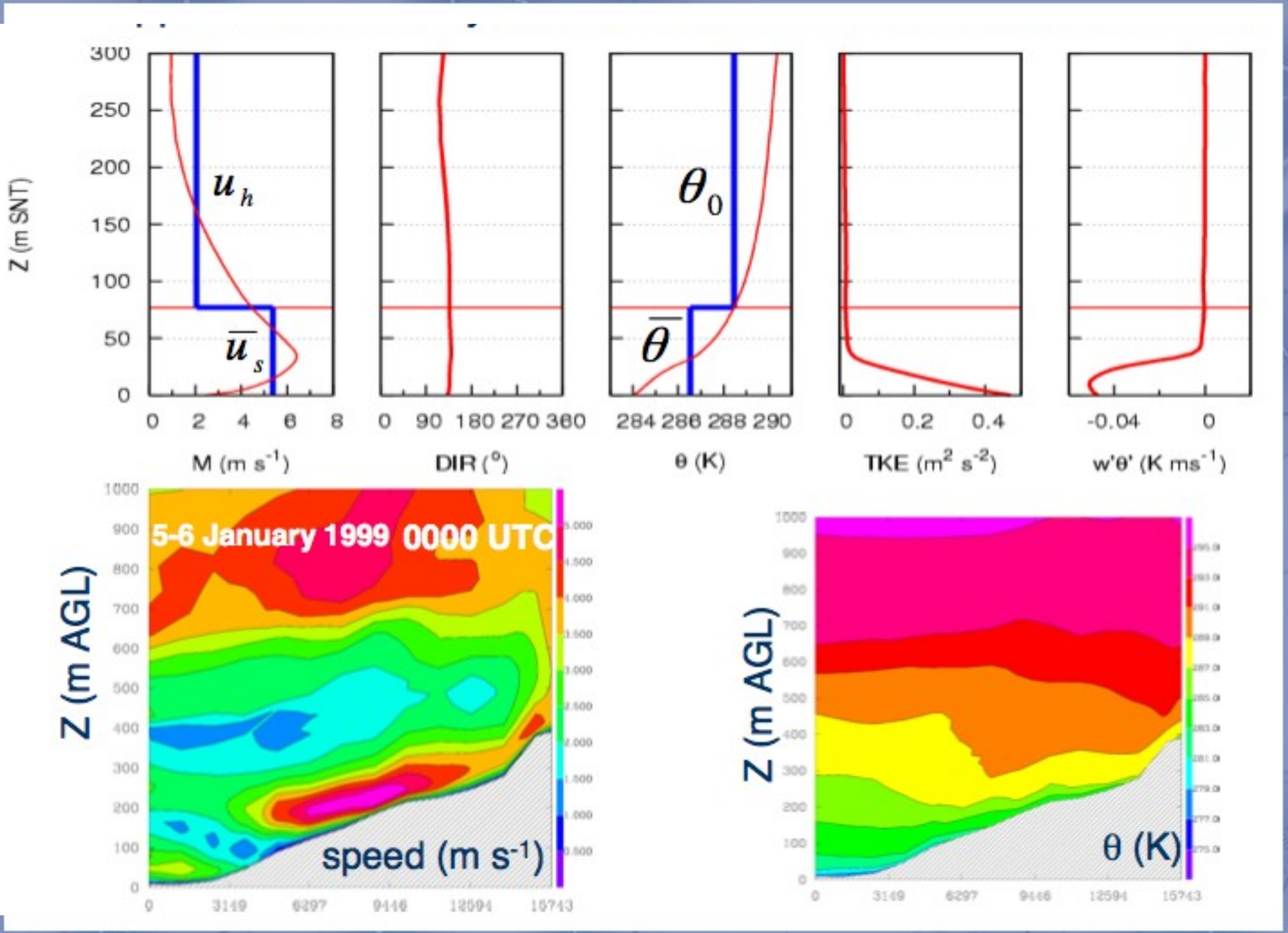

Source: Martinez and Cuxart 2007

Sloping terrain (4)

Momentum budget equation

$$\frac{\partial u_k}{\partial t} = F_{adv} + F_b + F_{\Delta\theta_k} + F_h + F_{cor} + F_{div}$$

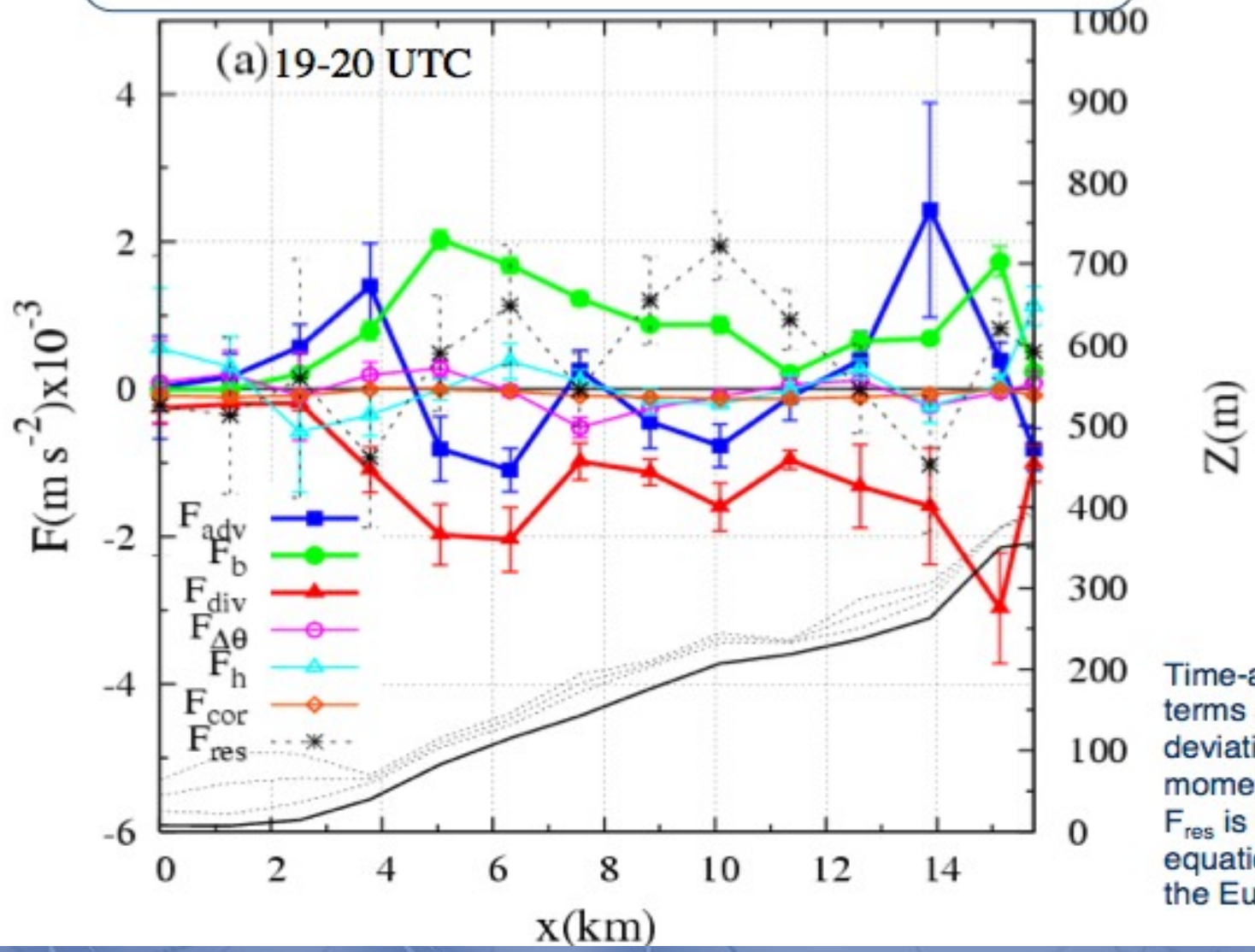

Time-averaged forcing terms and standard deviation from the momentum equation. F_{res} is the residual of the equation, also including the Eulerian acceleration.

Source: Martinez & Cuxart, 2007

Sloping terrain: other issues

a) LLJ height more significant for surface layer fluxes than L (Grisogono et al, 2007)

b) Accelerations due to changes in slope of
  i) angle (Skyllingstad, 2003)
  ii) surface T (Shapiro and Fedorovich, 2008)

c) Vegetation (Lee and Mahrt, 2006; Yi et al, 2005)

d) Interactions flow-topography

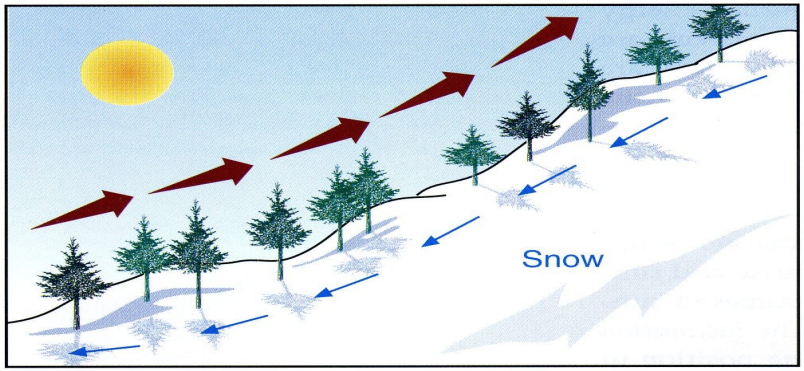

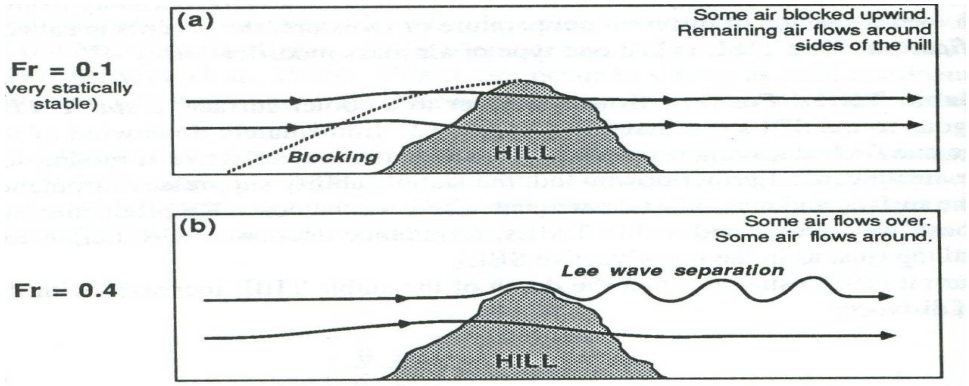

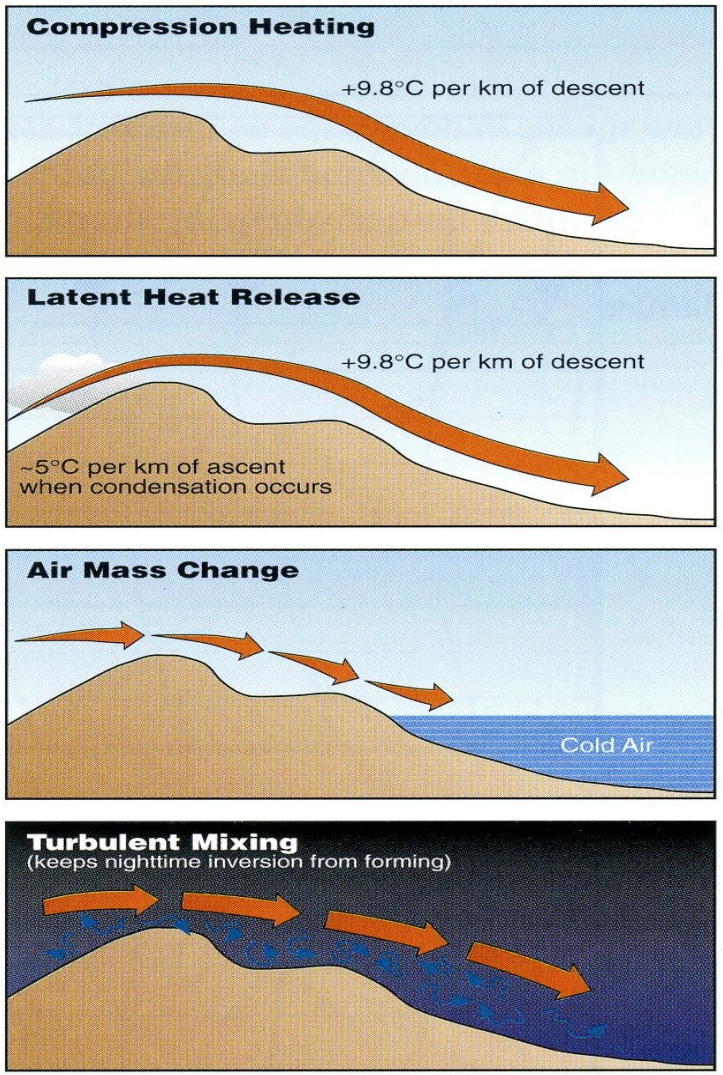

Figure 10.14 Four factors cause the warming and drying associated with chinooks. (Adapted from Beran, 1967)

Figures from Whiteman (2000), Hunt (1980)

Cold Pools (1)

Three basic types: different T evolutions

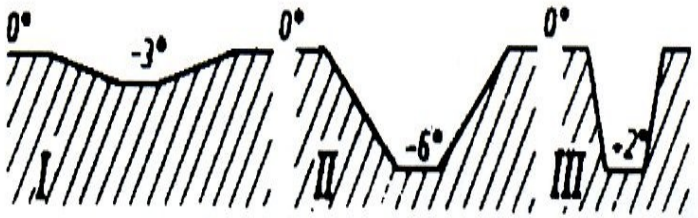

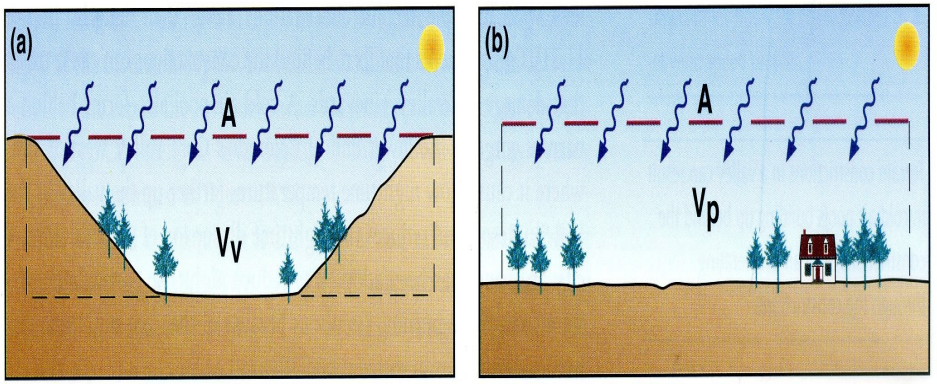

Topographic Amplification Factor (Whiteman 1990)

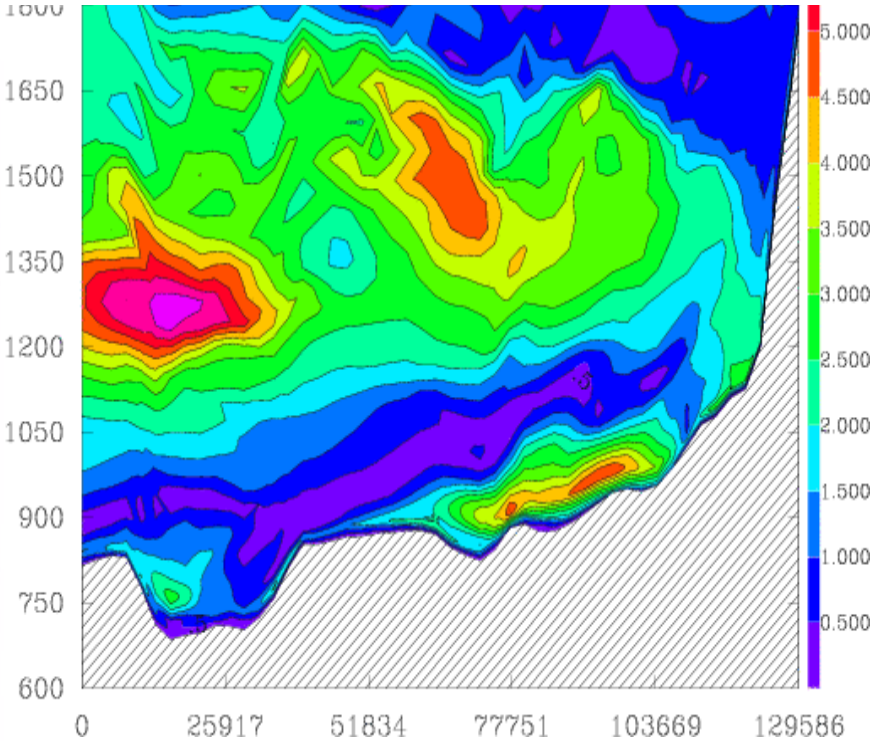

Long Downslope flow in the Duero basin

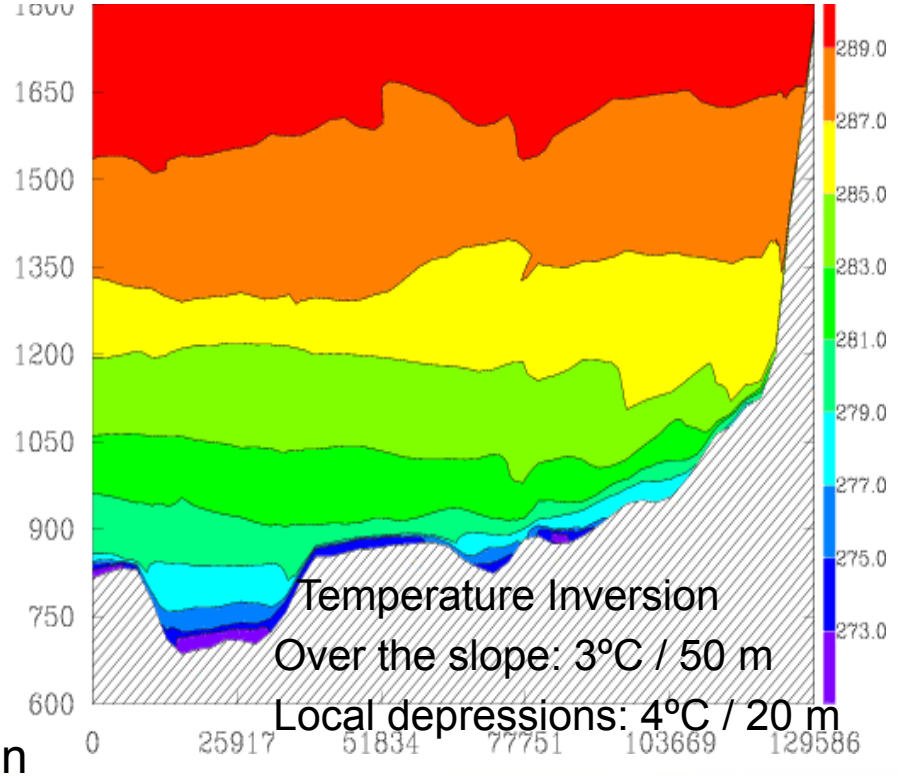

Temperature Inversion
Over the slope: 3ºC / 50 m
Local depressions: 4ºC / 20 m

Sources: Geiger (1995), Martinez and Cuxart (2009)

Hovmöller diagrams(18 to 6 LT) for slope and valley bottom (20 km distant)

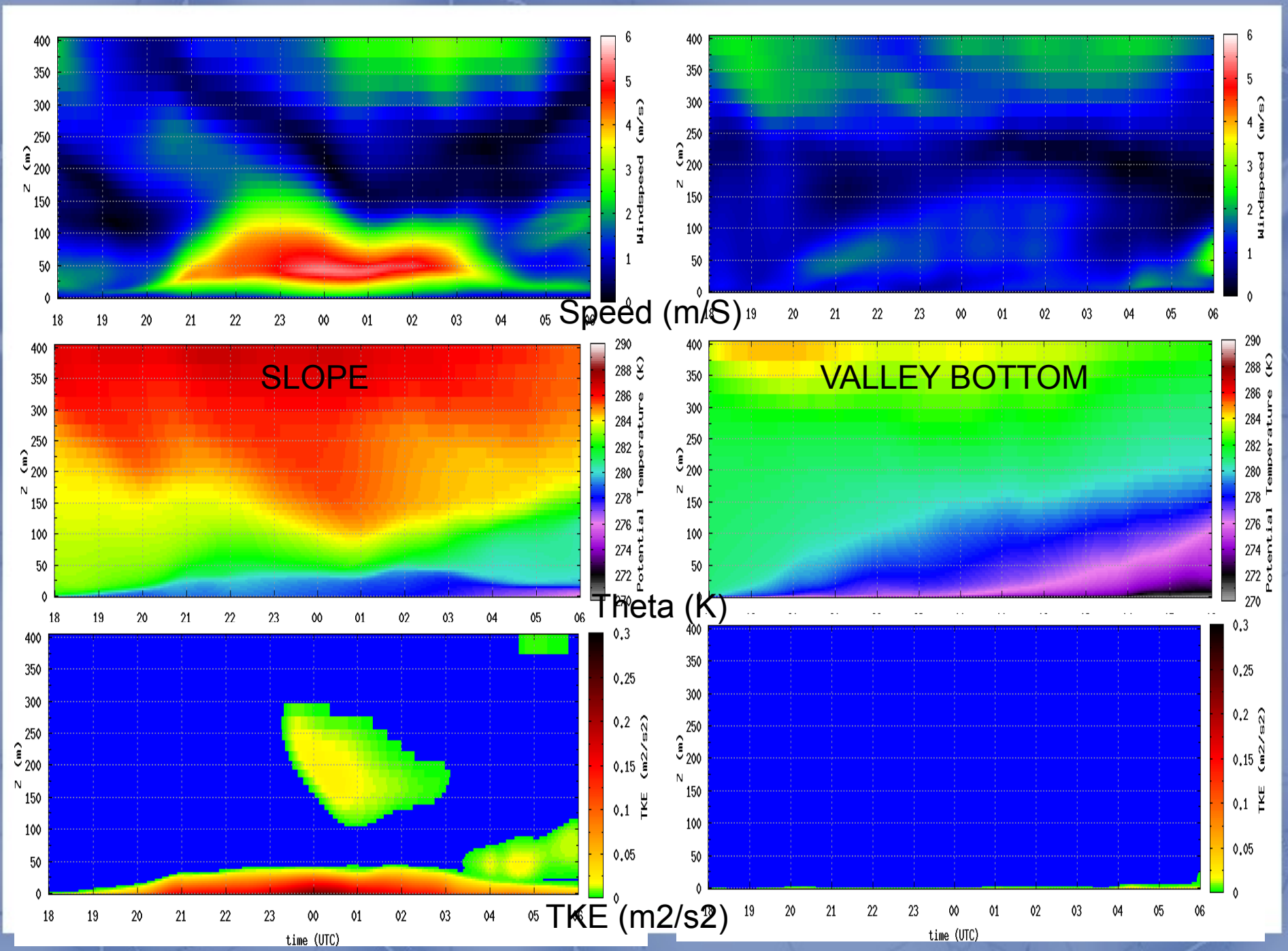

Source: Martinez & Cuxart, 2009

Cold Pools (3)

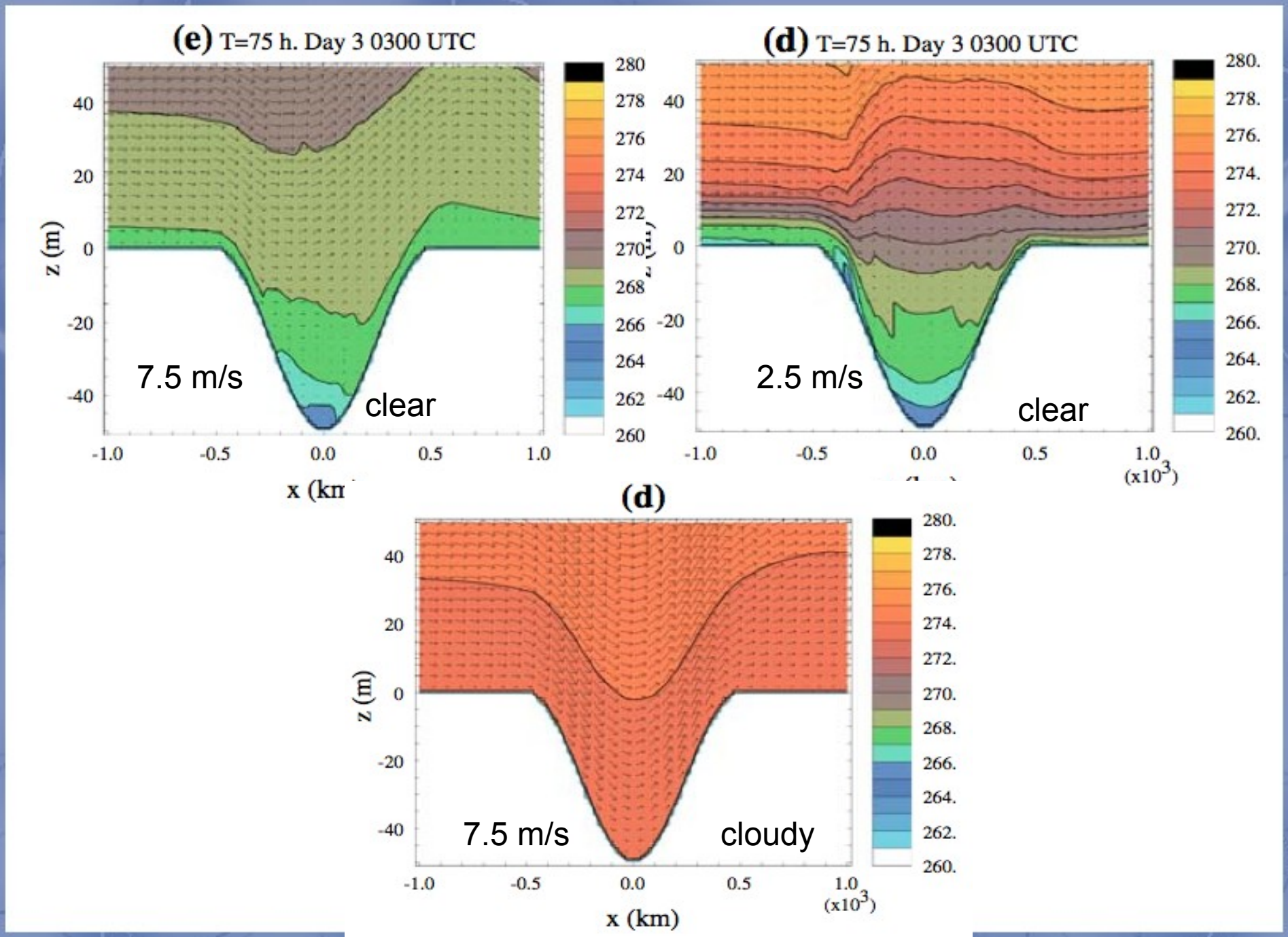

(Vosper & Brown, 2008)

Cold Pools (4)

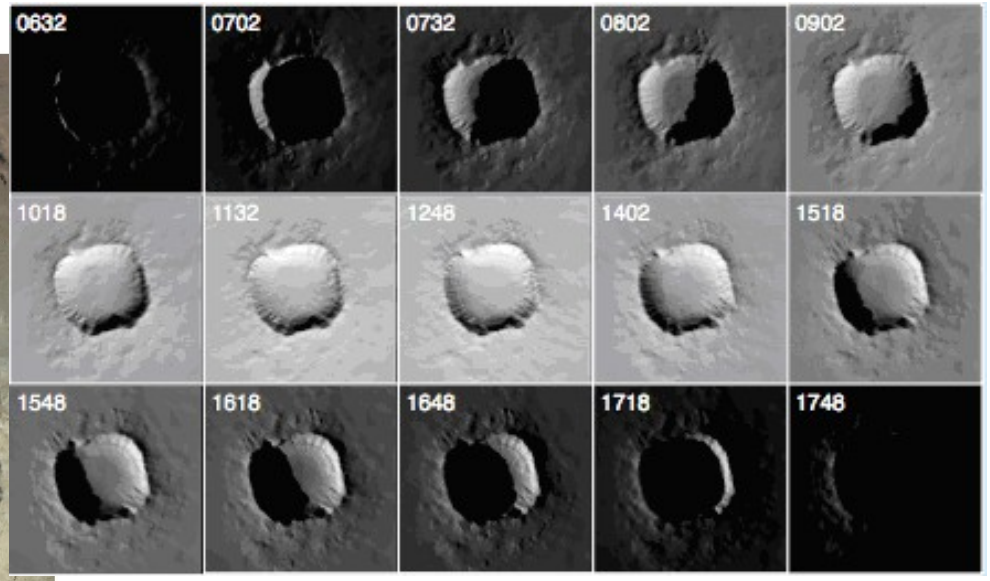

METCRAX 2006
(Whiteman et al, 2008)

Valley-Plain winds (1)

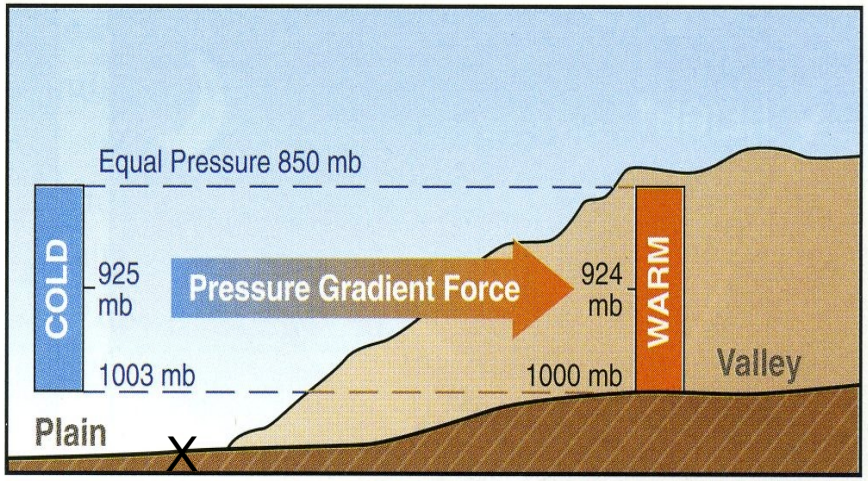

Daytime

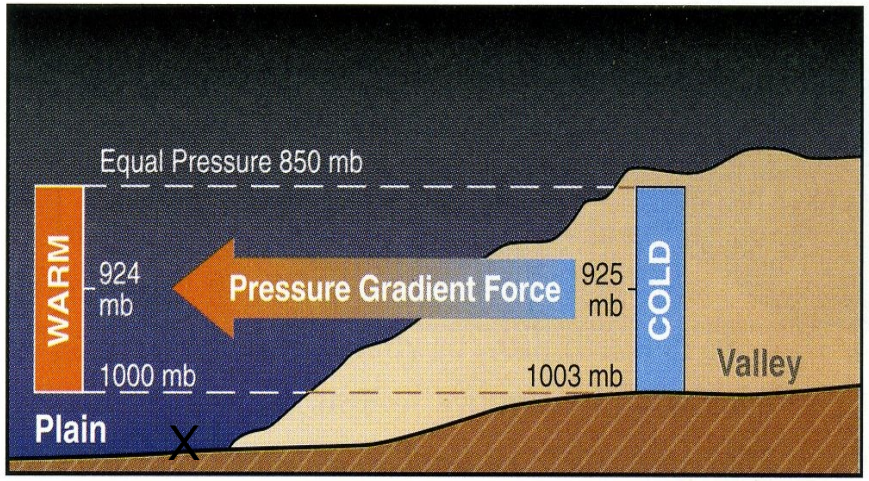

Nighttime

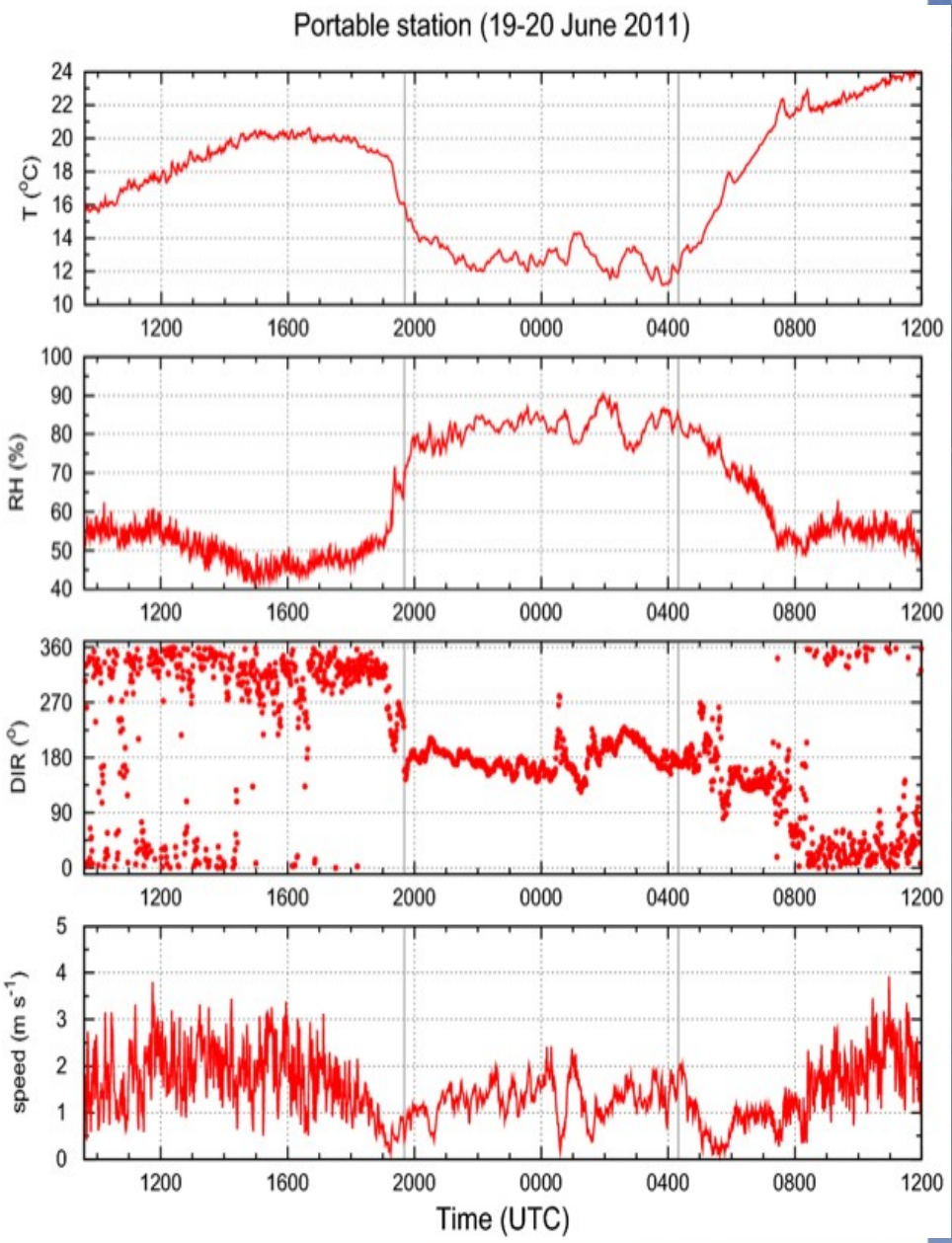

Sources: Whiteman (2000), UIB-BLLAST (2011)

Valley-Plain winds (2)

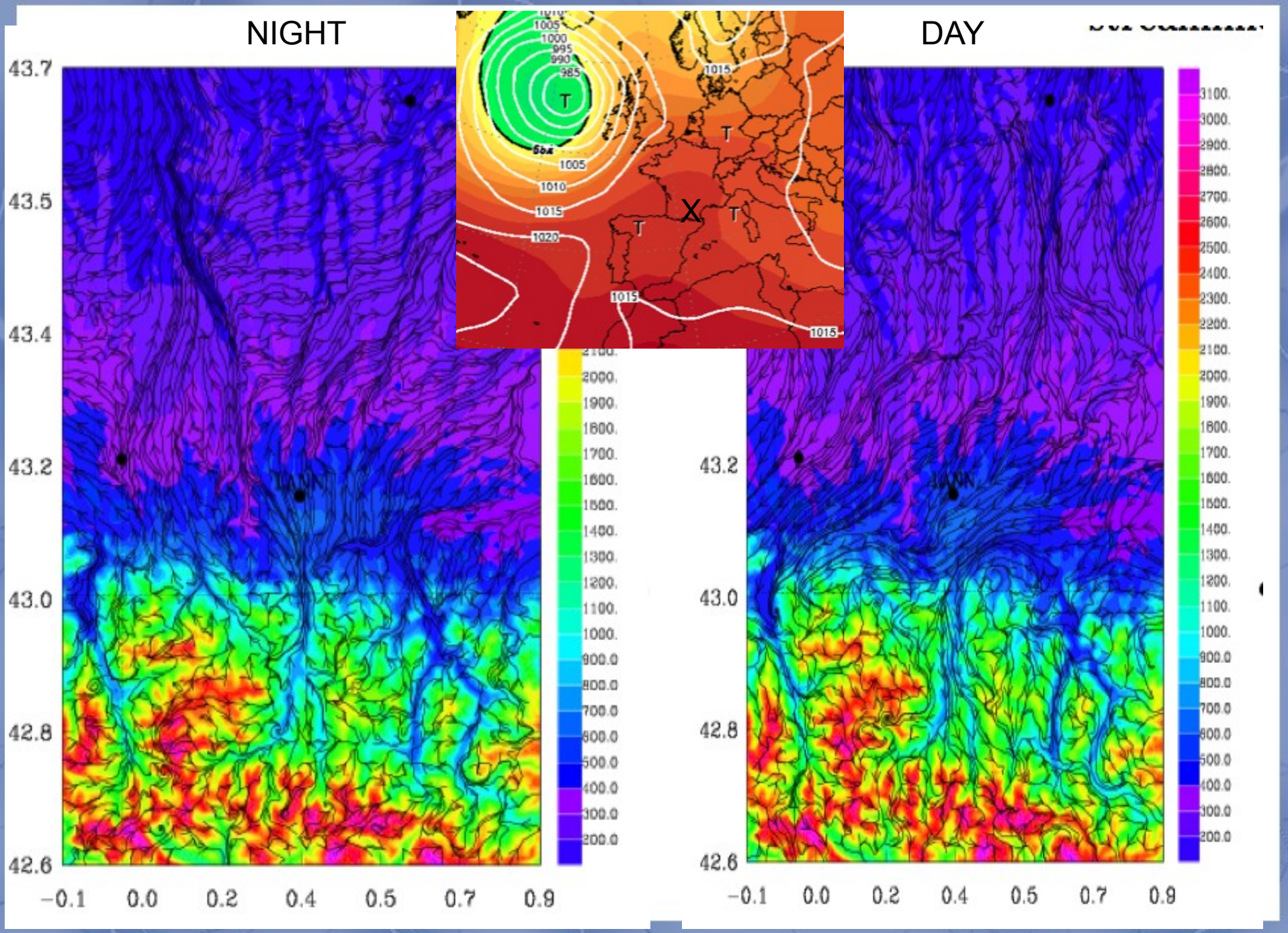

Valley-Plain winds (3)

Vertical cross-sections along the Aure valley

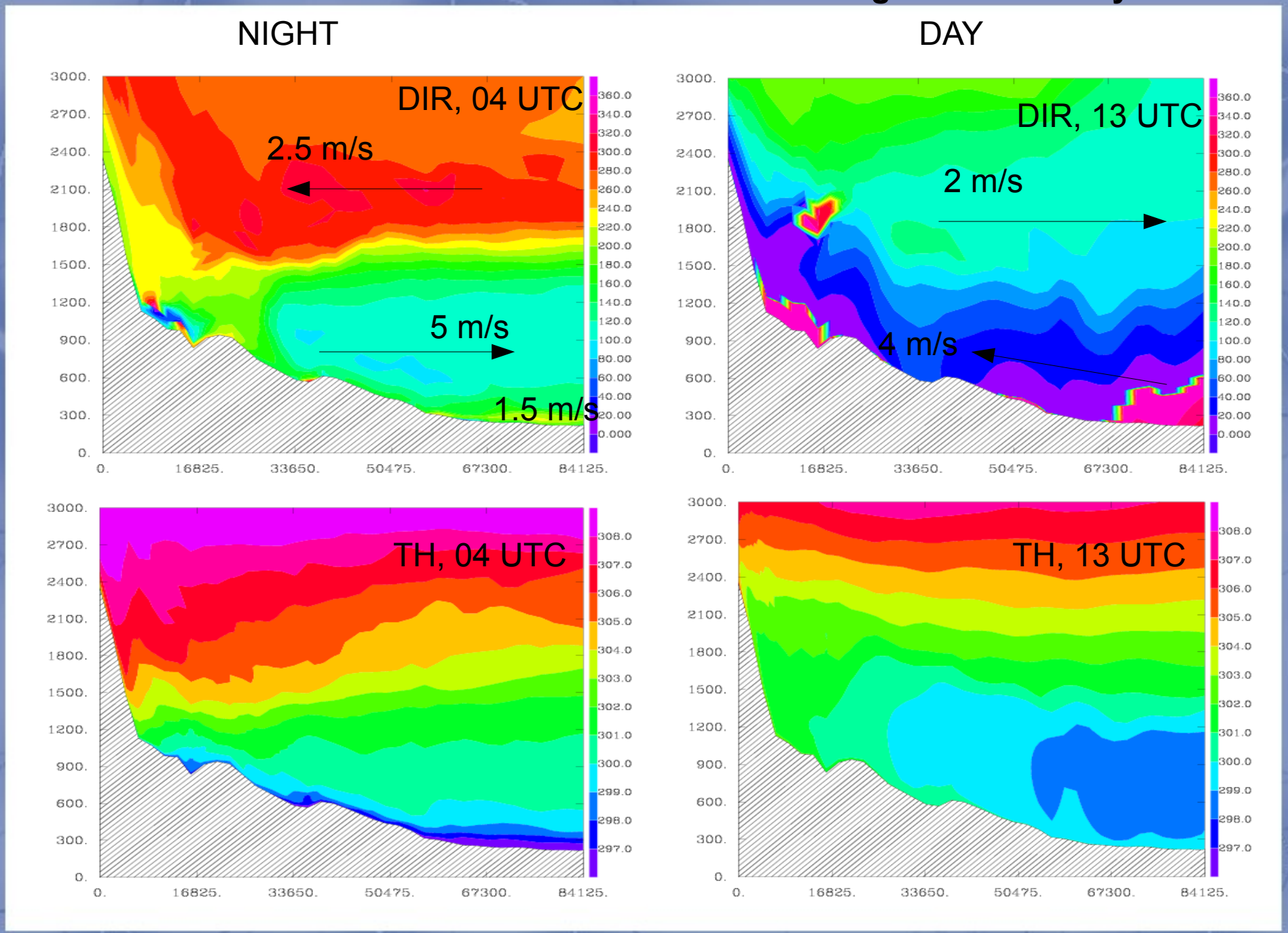

Source: UIB (Mallorca & Bergen, 2011)

Basin Heterogeneity

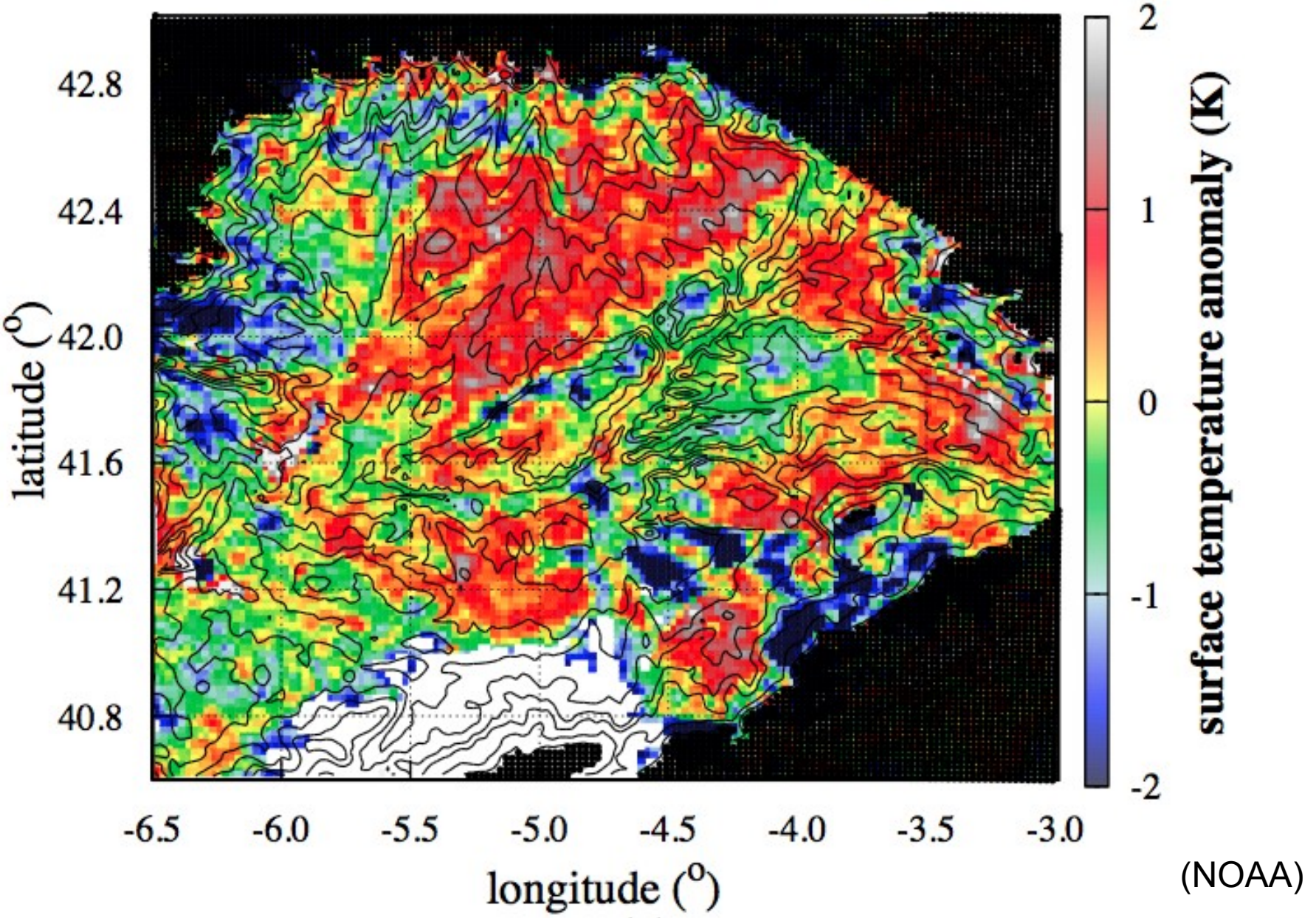

Source: Jimenez and Cuxart (2012, submitted)

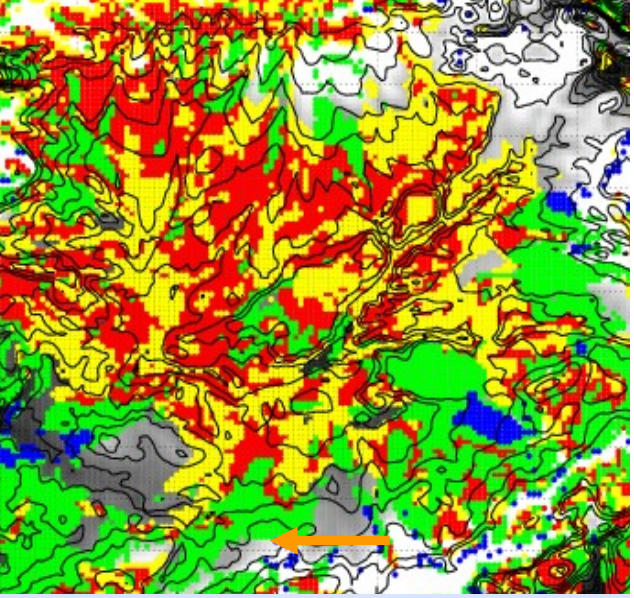

weak/moderate/strong/no jet

Table 1 Percentage of the cases (19430 in total) for the classification of the points at 0000 UTC according to the wind maxima (up to 100 m) and the temperature gradient (up to 10 m where $\Delta\theta = \theta_{10.5m} - \theta_{1.5m}$). The jet category is counted when the wind above the jet is, at least, 0.5 m s^{-1} smaller than in the jet height.

	$\Delta\theta < 0$ K	$0 \le \Delta\theta < 2$ K	$2 \le \Delta\theta < 4$ K	$\Delta\theta \ge 4$ K	Total
weak jet ($0.5 \le wind_{max} < 2$ m s^{-1})	0.04	18.08	6.85	1.02	**25.99**
moderate jet ($2 \le wind_{max} < 4$ m s^{-1})	0.02	21.98	2.17	0.25	**24.42**
strong jet ($wind_{max} > 4$ m s^{-1})	0.00	2.30	0.07	0.00	**2.37**
no jet-weak ($wind_{below100m} < 2$ m s^{-1})	0.08	12.10	8.32	2.05	**22.55**
no jet-moderate ($wind_{below100m} \ge 2$ m s^{-1})	0.12	20.45	3.29	0.81	**24.67**
total	**0.26**	**74.91**	**20.70**	**4.13**	100.00

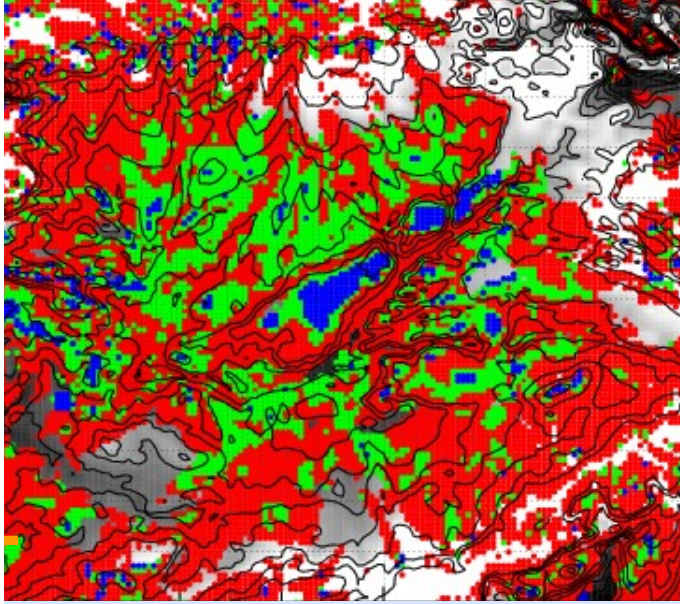

Weak/moderate/Strong st.

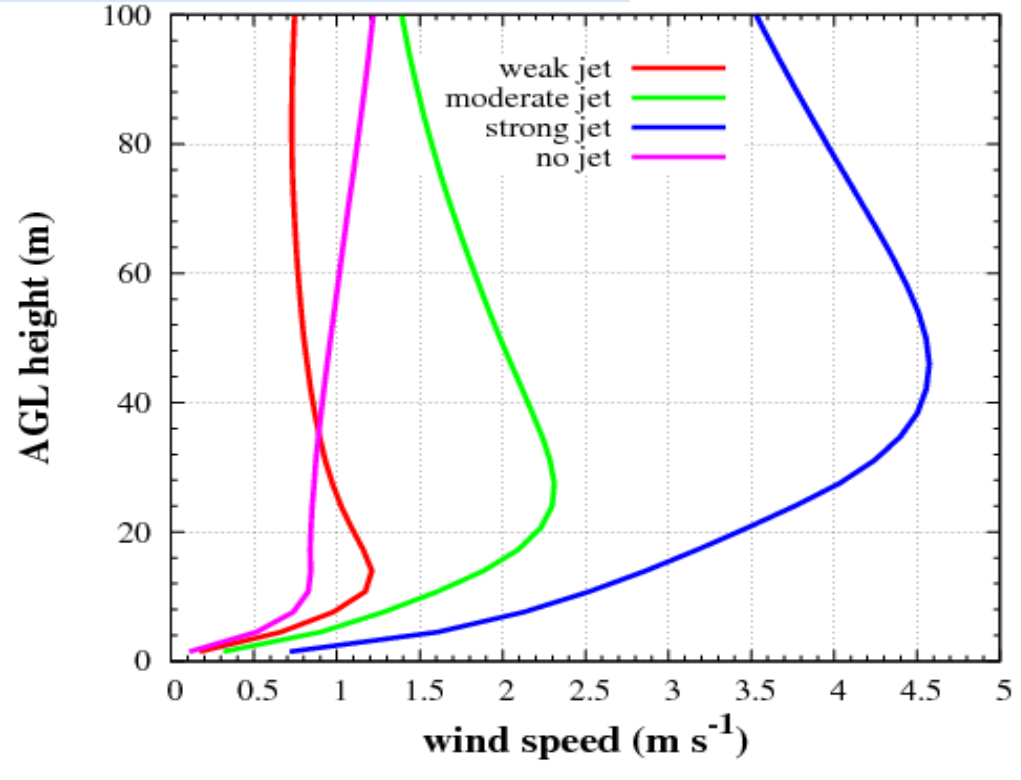

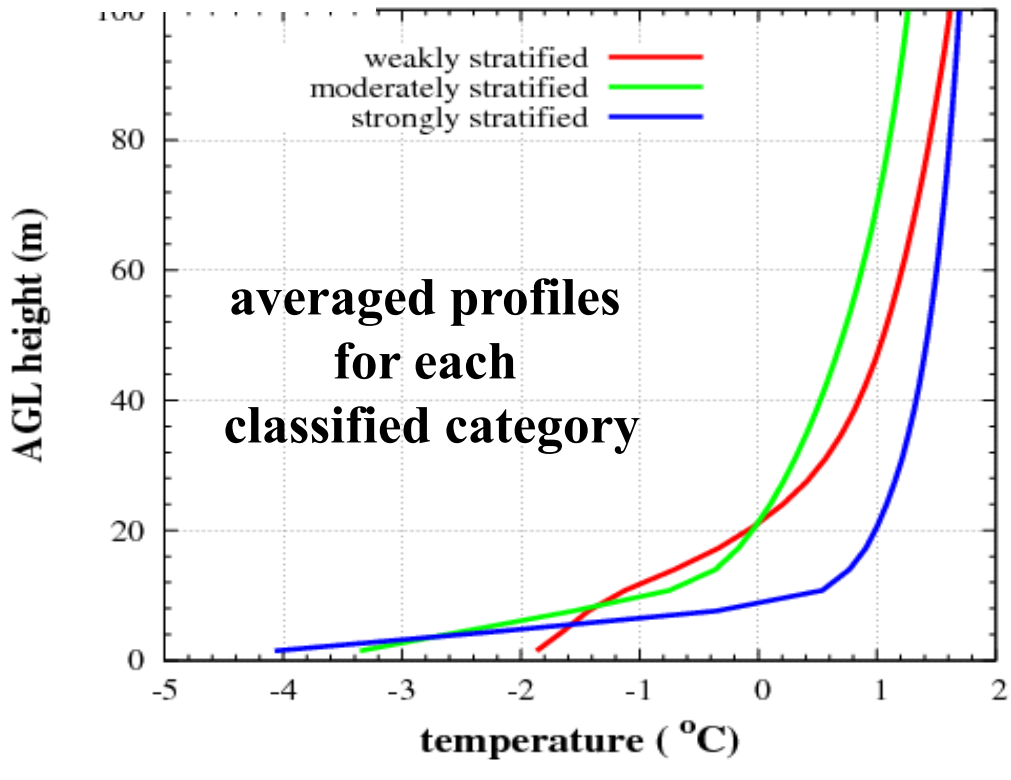

Source: Martinez et al, BLM, 2010

Within-basin mesoscale thermal heterogeneities: Ebro basin

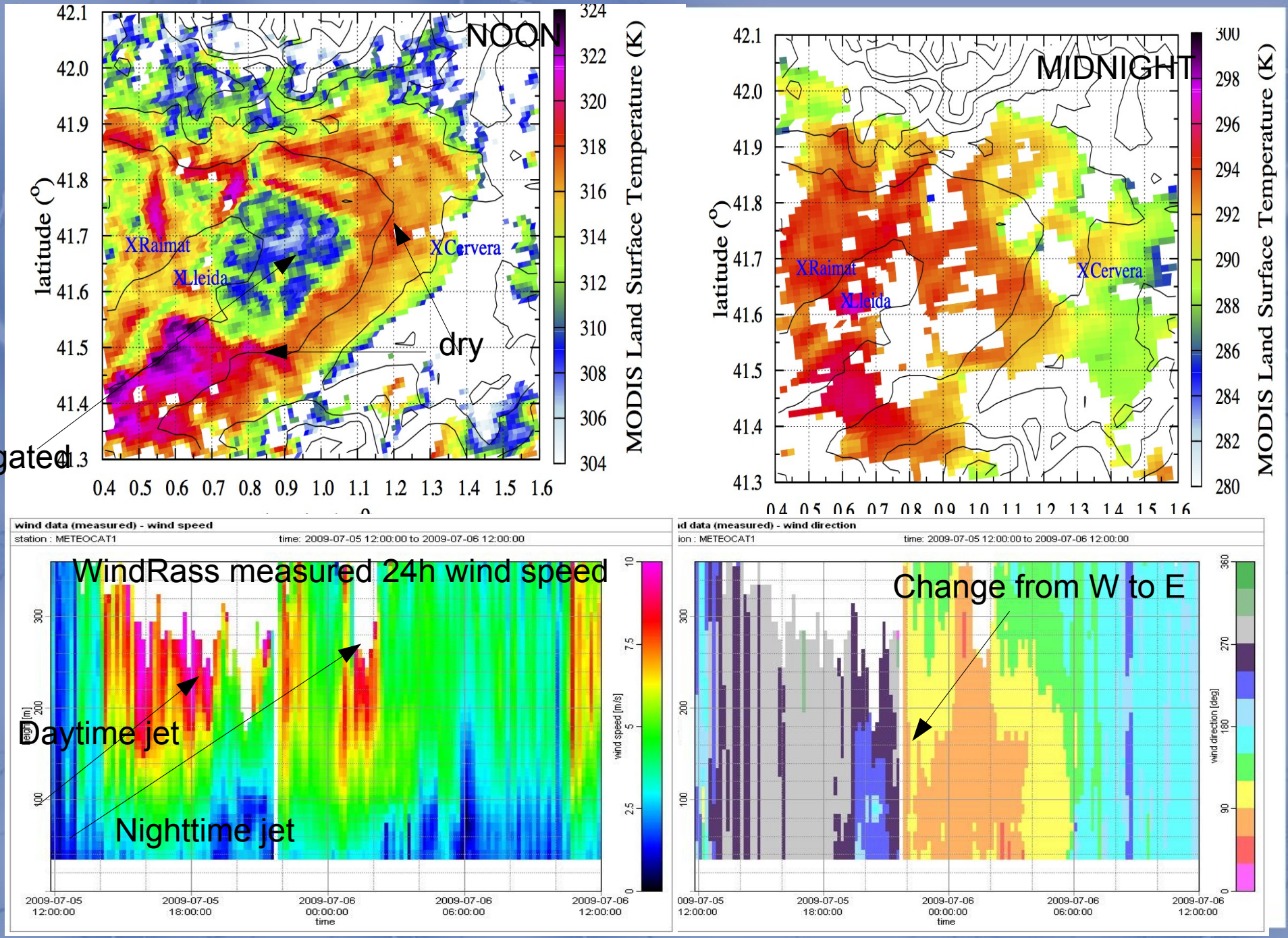

Cuxart et al, BLM, 2011

36-h fog in a wide closed basin (Ebro)

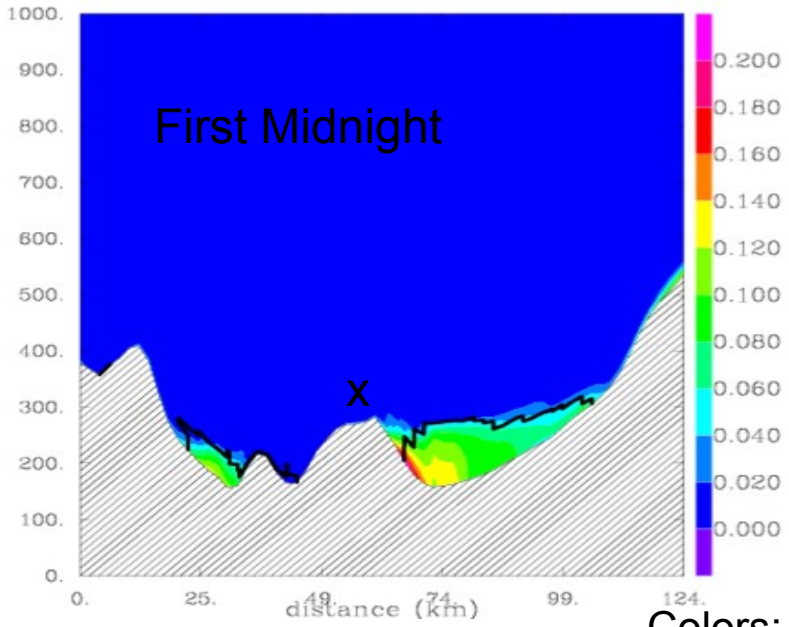

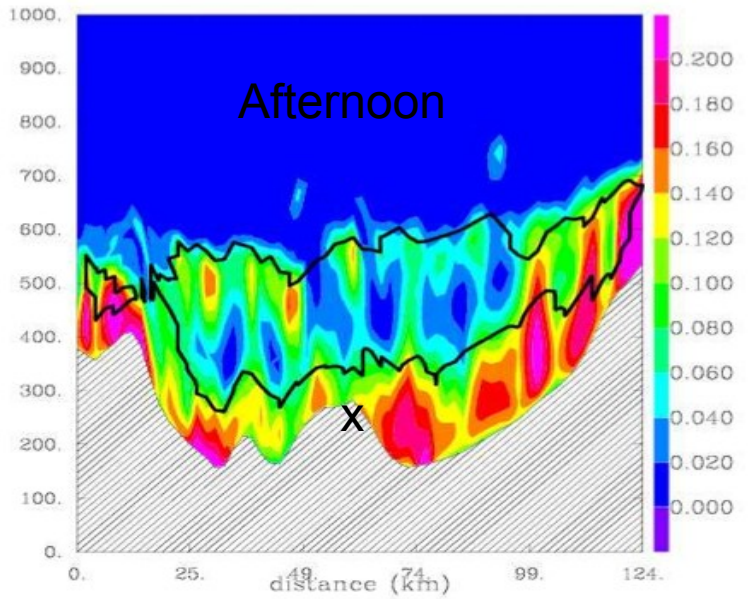

Colors: TKE; Black line: limits of the fog layer

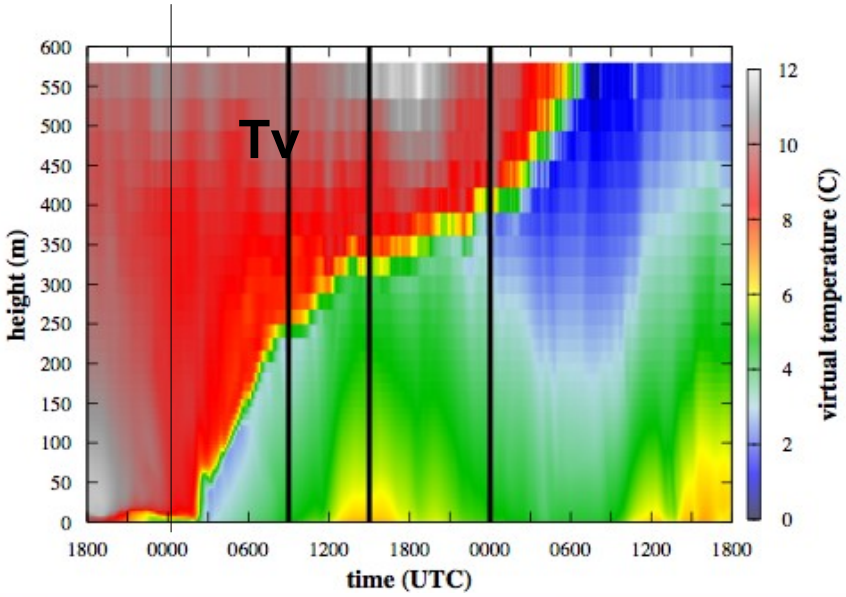

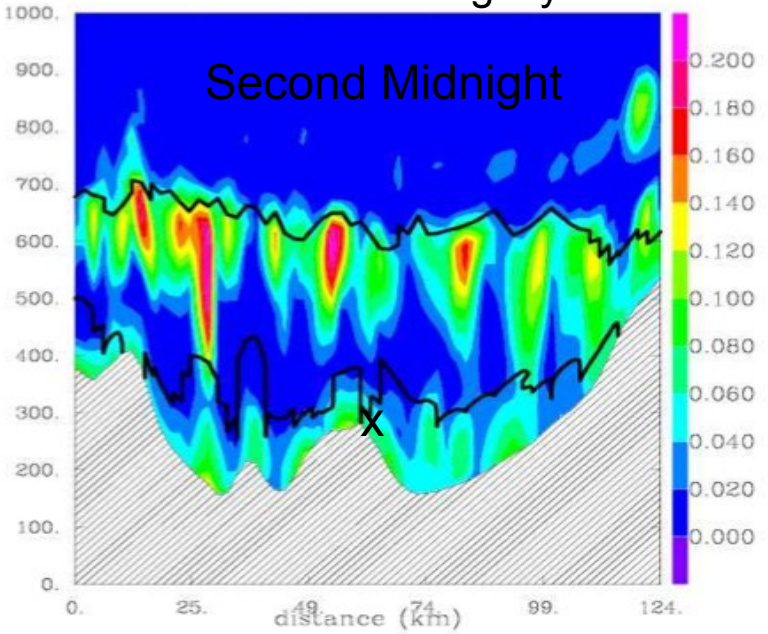

Cuxart & Jimenez, PAG, 2011

A possible summary :

* Land ABL is over complex terrain

* Low-level jets are a very common feature and oppose to the formation of very strong temperature inversions

* It is difficult to comprehend our measurements without a general understanding of the effects of the varying surrounding terrain

* High-resolution models can capture the main features related to topography

* To understand these features we must design very carefully our runs

* Effort must be put on the proper representation of the changing lower BC

Acknowledgements: to my colleagues at UIB M-A. Jiménez and Dani Martínez
Funding: Spanish Ministry of Science, grant CGL2009-12797-C03-01